NBS TECHNICAL NOTE 1032

U.S. DEPARTMENT OF COMMERCE / National Bureau of Standards

Measurement of Far-Field and Near-Field Radiation Patterns from Optical Fibers

NATIONAL BUREAU OF STANDARDS

The National Bureau of Standards[1] was established by an act of Congress on March 3, 1901. The Bureau's overall goal is to strengthen and advance the Nation's science and technology and facilitate their effective application for public benefit. To this end, the Bureau conducts research and provides: (1) a basis for the Nation's physical measurement system, (2) scientific and technological services for industry and government, (3) a technical basis for equity in trade, and (4) technical services to promote public safety. The Bureau's technical work is performed by the National Measurement Laboratory, the National Engineering Laboratory, and the Institute for Computer Sciences and Technology.

THE NATIONAL MEASUREMENT LABORATORY provides the national system of physical and chemical and materials measurement; coordinates the system with measurement systems of other nations and furnishes essential services leading to accurate and uniform physical and chemical measurement throughout the Nation's scientific community, industry, and commerce; conducts materials research leading to improved methods of measurement, standards, and data on the properties of materials needed by industry, commerce, educational institutions, and Government; provides advisory and research services to other Government agencies; develops, produces, and distributes Standard Reference Materials; and provides calibration services. The Laboratory consists of the following centers:

Absolute Physical Quantities[2] — Radiation Research — Thermodynamics and Molecular Science — Analytical Chemistry — Materials Science.

THE NATIONAL ENGINEERING LABORATORY provides technology and technical services to the public and private sectors to address national needs and to solve national problems; conducts research in engineering and applied science in support of these efforts; builds and maintains competence in the necessary disciplines required to carry out this research and technical service; develops engineering data and measurement capabilities; provides engineering measurement traceability services; develops test methods and proposes engineering standards and code changes; develops and proposes new engineering practices; and develops and improves mechanisms to transfer results of its research to the ultimate user. The Laboratory consists of the following centers:

Applied Mathematics — Electronics and Electrical Engineering[2] — Mechanical Engineering and Process Technology[2] — Building Technology — Fire Research — Consumer Product Technology — Field Methods.

THE INSTITUTE FOR COMPUTER SCIENCES AND TECHNOLOGY conducts research and provides scientific and technical services to aid Federal agencies in the selection, acquisition, application, and use of computer technology to improve effectiveness and economy in Government operations in accordance with Public Law 89-306 (40 U.S.C. 759), relevant Executive Orders, and other directives; carries out this mission by managing the Federal Information Processing Standards Program, developing Federal ADP standards guidelines, and managing Federal participation in ADP voluntary standardization activities; provides scientific and technological advisory services and assistance to Federal agencies; and provides the technical foundation for computer-related policies of the Federal Government. The Institute consists of the following centers:

Programming Science and Technology — Computer Systems Engineering.

[1]Headquarters and Laboratories at Gaithersburg, MD, unless otherwise noted; mailing address Washington, DC 20234.
[2]Some divisions within the center are located at Boulder, CO 80303.

Measurement of Far-Field and Near-Field Radiation Patterns from Optical Fibers

Ernest M. Kim
Douglas L. Franzen

Electromagnetic Technology Division
National Engineering Laboratory
National Bureau of Standards
Boulder, Colorado 80303

U.S. DEPARTMENT OF COMMERCE, Malcolm Baldrige, Secretary

NATIONAL BUREAU OF STANDARDS, Ernest Ambler, Director

Issued February 1981

NATIONAL BUREAU OF STANDARDS TECHNICAL NOTE 1032
Nat. Bur. Stand. (U.S.), Tech. Note 1032, 48 pages (Feb. 1981)
CODEN: NBTNAE

U.S. GOVERNMENT PRINTING OFFICE
WASHINGTON 1981

For sale by the Superintendent of Documents, U.S. Government Printing Office, Washington, D.C. 20402

Price $2.50 (Add 25 percent additional for other than U.S. mailing)

CONTENTS

MEASUREMENT OF FAR-FIELD AND NEAR-FIELD RADIATION PATTERNS FROM OPTICAL FIBERS

Ernest M. Kim* and Douglas L. Franzen

Systems are described for measuring the far- and near-field radiation patterns from optical fibers. Parameters which affect measurement precision, accuracy, resolution, and signal-to-noise ratio are discussed. Measurements utilizing radiation patterns are covered; this includes radiation angle (numerical aperture), attenuation using mode filters, index profile, core diameter, and mode volume transfer function. Experimental examples are given in many instances.

Key words: Attenuation; core diameter; far field; index profile; mode filter; numerical aperture; radiation angle; radiation patterns.

1. INTRODUCTION

Radiation patterns exiting optical fibers yield important information used in fiber specification. For example, in some instances core diameter and numerical aperture are obtained from radiation patterns. Measurement practices with regard to these parameters continue to evolve as accumulated practical experience and the efforts of standards groups lead toward uniformly accepted procedures. This Technical Note is one of a series intended to describe the present design and capabilities of fiber measurement systems used at the National Bureau of Standards. These systems are perhaps representative of current practice in the industry and many of the present techniques and methods will be relevant to future systems.

2. RADIATION PATTERN CONSIDERATIONS IN OPTICAL FIBERS

The radiation propagating in an optical fiber can take on various spatial and angular distributions depending upon the relative excitation of fiber modes. Useful information about the fiber can be obtained by analyzing the radiation exiting an end. This analysis can take place in either the far- or near-field region of the end. A far-field measurement determines the angular dependence of intensity (irradiance) sufficiently far from the end of the fiber (fig. 2-1); whereas, a near-field measurement determines the spatial intensity distribution in the plane of the end face.

In the far-field, the normalized, angular intensity distribution no longer depends on distance from the fiber. While the intensity at any given angular coordinate decreases as the square of the distance from the fiber end, the normalized pattern remains constant. If the far-field pattern is circularly symmetric about the fiber axis, then a single angular coordinate is sufficient to describe the pattern.

The far-field, which is synonymous with the Fraunhoffer diffraction region, is usually said to start at a distance

*NBS Coop graduate student on leave from New Mexico State University, Las Cruces, NM.

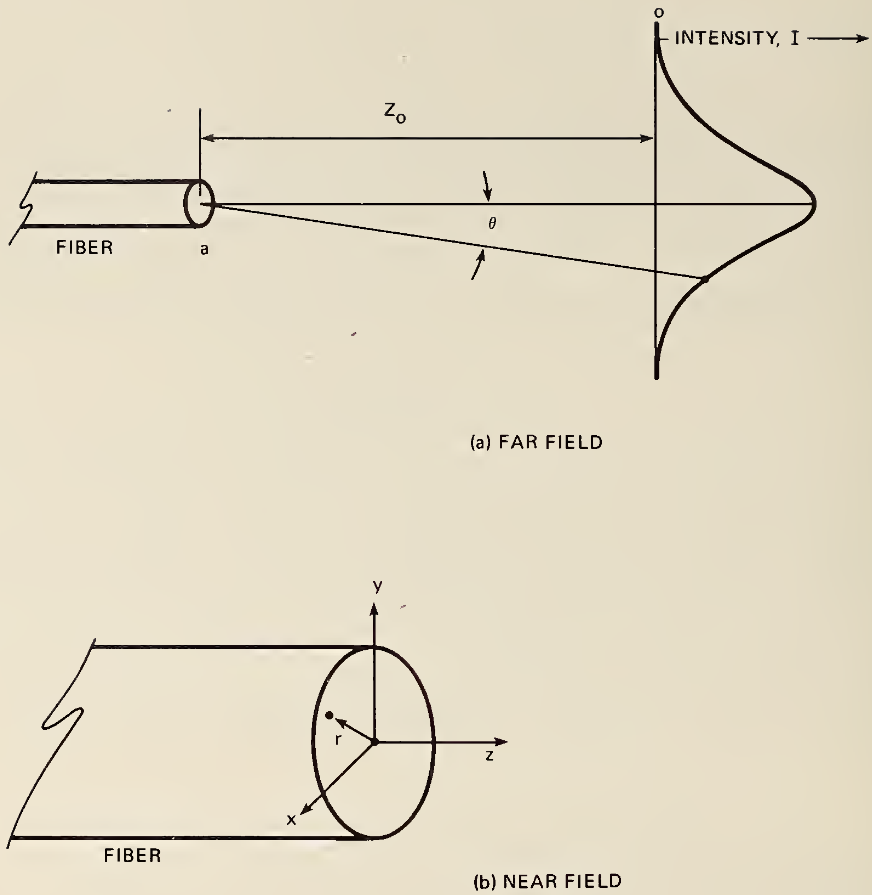

igure 2-1. Radiation pattern measurements from optical fibers, (a) far field is given by $I(\theta)$ at $z >> z_0$, (b) near field is given by $I(r)$ in xy plane.

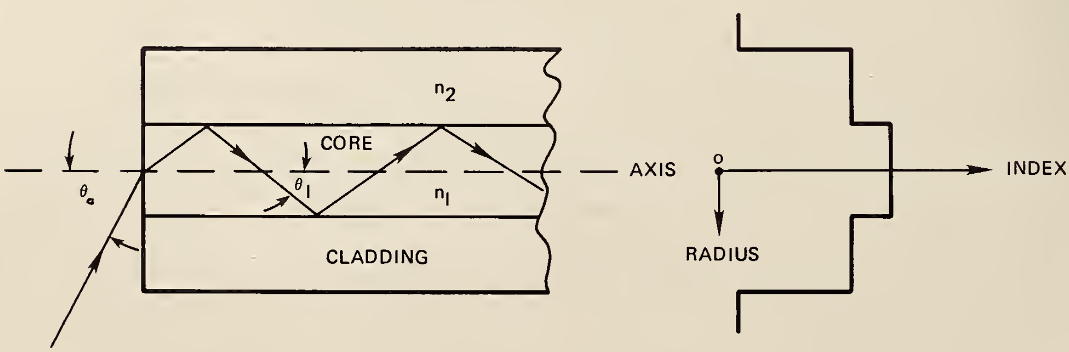

igure 2-2. The meridional ray in a step index fiber making the maximum possible angle, θ_l, with the fiber axis.

$$z_0 = \frac{(2a)^2}{\lambda} \tag{1}$$

from the fiber end, where λ is the wavelength of light and a the core radius [1]. When $z \gg z_0$, the amplitude (electric field) distribution in the far-field is closely related to the spatial Fourier transform of the amplitude distribution existing at $z = 0$, [1]. In practice, far-field measurements are made at distances greater than 10 z_0 from the fiber end. For the standard graded index core diameter of 50 μm and a wavelength of 1 μm, 10 z_0 is 2.5 cm. For the standard step index core diameter of 100 μm, the distance becomes 10 cm. Both of these lengths represent convenient laboratory working distances.

Radiation patterns are measured on either short or long lengths of fiber, depending upon the application. Frequently the short length is a 2 m cutback length left over from an attenuation or bandwidth measurement. In this Technical Note, a long length refers to the entire length of fiber under test and, for telecommunications fibers, generally exceeds 1 km.

Radiation patterns depend upon launching conditions and contain contributions from both guided and tunneling leaky modes of the fiber [2,3]. In short lengths, patterns result mainly from guided modes with a significant contribution from leaky modes. The relative importance of the leaky mode contribution depends upon the index profile and launching conditions. In long lengths, leaky modes have generally decayed and the patterns result from guided modes modified by differential mode attenuation and mode coupling. Far- and near-field patterns resulting from overfilled launching conditions on graded index fibers generally become restricted with further propagation along the fiber. This occurs because differential mode attenuation is generally higher for higher order modes. Eventually an equilibrium is reached between mode coupling and differential mode attenuation to yield a steady state pattern. However, steady state is seldom observed in practice since mode coupling lengths in good fibers are several kilometers [4] if not tens of kilometers [5].

The remainder of this section briefly discusses the measurement applications of far- and near-field patterns. Various applications are summarized in table I. For some of these measurements, procedures are pending before standards groups [6]. In general, more attention has been given to standardizing procedures for graded index fibers than for step index fibers.

Table I
Measurement Applications of Radiation Patterns from Multimode Fibers

Application	Fiber length employed Short (2 m)	Long	Radiation pattern Far field	Near field	Launching condition	General comments
1 Radiation Angle (Numerical aperture)	X		X		Overfill	Meridionally defined NA approximated for near parabolic graded index fibers. Special considerations necessary for step index.
2 Attenuation using restricted launch via a mode filter	X	X	X		Overfill	Used to qualify mode filters; applies to graded index fibers over 1 km in length.
3 Index profile	X			X	Overfill	Little or no leaky mode correction required for near parabolic graded index fibers; large correction for step index. Limited resolution, information on guiding regions of fiber only.
4 Core diameter	X			X	Overfill	Possible uncertainty due to low index "barrier" layer, poor resolution near core-cladding boundary, may have problems conforming to an index profile definition of core diameter, is easy to implement.
5 Mode volume transfer function	X	X	X	X	Restricted	Applies to graded index fibers, measurement system must have ability to control launch mode volume and therefore beam optics systems capable of independently variable launch spot and NA are usually required.

2.1 Measurements Utilizing Far-Field Patterns

2.1.1 Radiation Angle (Numerical Aperture)

The cone of light rays accepted by a fiber is of practical importance. Launching efficiency of sources like LEDs and loss performance of joined sections of dissimilar fiber depend upon this parameter. "Radiation angle" is a measure of the cone angle transmitted by the fiber [7]. This measurement is usually made in the far field of a short, 2 m length excited at a specified wavelength using overfilled launching conditions; i.e., constant irradiance over the core with a launch angle greatly exceeding the fiber acceptance angle.

In early fiber work, the cone angle containing 90 percent of the transmitted power was determined by either integrating a far-field intensity pattern or by translating an aperture in the far field. The sine of the half angle of this cone was frequently termed "90 percent numerical aperture."

More recent procedures pending before standards groups define radiation angle directly from a far-field intensity pattern [8]. In this instance, radiation angle is defined as the half angle where the far-field intensity has decreased to 5 percent of the peak value. The sine of this angle, for near parabolic index multimode fibers, is close to the index defined numerical aperture.

Historically, the term "numerical aperture" (NA) has been used to describe the largest angle meridional ray accepted by a fiber, figure 2-2, with

$$NA \equiv \sin \theta_0 = \sqrt{n_1^2 - n_2^2} \tag{2}$$

$$= n_1\sqrt{2\Delta} \text{ with } \Delta \approx \frac{n_1-n_2}{n_1} \tag{3}$$

where n_1 is the core index of refraction, n_2 the cladding index, and Δ is defined by the above equations. While figure 2-2 applies to step fibers, analysis shows that the numerical aperture of graded index fibers is also given by eq (2) with n_1 being the on-axis index of refraction [9].

The sine of the radiation angle based on the 5 percent intensity points is close to the index defined NA of eq (2) for near parabolic index fibers. Theoretical work shows the acceptance angle of skew rays is always less than that of meridional rays in near parabolic index fibers [10]. Adams, et al., show that leaky modes in a near parabolic index fiber are all contained within the meridionally defined numerical aperture [3]. Thus, when all modes are excited, the largest observed angle in a far-field pattern would be given by θ_0 in eq (2). At the 5 percent level, patterns are close to the maximum observable angle.

For step fibers, the situation is quite different. Here the acceptance angles for skew rays can exceed θ_0. When all modes are excited, radiation would appear at angles greater than θ_0. Thus, to obtain the numerical aperture based on eq (2) for short step index fibers, special launching conditions would be necessary. This would probably mean launching only meridional rays. This could be accomplished by small spot excitation at core center.

2.1.2 Attenuation with Restricted Launch Via a Mode Filter

In measuring the attenuation of long telecommunications type fibers, it is useful to launch with a distribution which gives good concatenation predictions [11]. This is presently accomplished by restricting the launch to avoid the excitation of certain high loss modes which do not propagate far in the fiber. In general, this can be accomplished by one of two approaches. The beam optics approach avoids the initial excitation of certain high loss modes by restricting the launch spot size and numerical aperture at the fiber input end. (70 percent of the core diameter at 70 percent of the fiber NA is the choice pending before standards groups.) In the mode filter approach, the fiber is initially overfilled and a mode filter is applied to strip out certain high loss modes.

Far-field radiation pattern measurements on long and short fiber lengths are used to qualify a mode filter for an attenuation measurement. Current proposals call for overfilling the input of the fiber under test in both spot size and numerical aperture, then measuring the radiation angle (5 percent intensity) exiting the long length. An appropriate mode filter is applied so the radiation angle exiting a 2 m length is less than that of the long length by 3 ± 3 percent. Now the mode filter has stripped away enough of the high angle-high loss modes to simulate, in a 2 m cutback length, the radiation pattern resulting from a kilometer or more of propagation. Common mode filters include dummy fibers and mandrel wraps [12], [13].

2.2 Measurements Utilizing Near-Field Patterns

2.2.1 Index Profile

When a multimode optical fiber having a large number of modes is uniformly illuminated to equally excite all bound modes, the near-field pattern approximates the refractive index profile of the core [14]. In short lengths where differential mode attenuation and mode coupling are negligible, the deviation from the index profile is due mainly to the presence of tunneling leaky modes. Sladen, et al., have derived a leaky mode correction factor allowing one to obtain the index profile from transmitted near-field data [2]. The radial index profile difference, $n(r) - n_2$, is given by

$$n(r) - n_2 \approx \frac{n(o)-n_2}{C(r,z)} \frac{P(r)}{P(o)} \tag{4}$$

where $n(r)$ is the index in the core, n_2 the cladding index, $P(r)$ the near-field intensity as a function of radius, and $C(r,z)$ the correction factor. $C(r,z)$ depends on the nominal profile shape, fiber length, and radial position. $C(r,z)$ is zero at the core center and gradually rises to a maximum near 0.9a, where a is the core radius. As an example [14], for a 1 m length of fiber having a near parabolic index profile, a core diameter of 80 μm, an NA of 0.18, and at a wavelength of 0.9 μm, the correction factor is 8 percent at 0.6 a, rising to 20 percent at 0.85 a.

Whether a leaky mode correction should be made for near parabolic profile, graded index fibers is still open to debate. Calculations by Petermann [15] indicate a slight core ellipticity can cause leaky modes to attenuate more rapidly than indicated in references [2] and [14] and corrections would not be necessary for practical near parabolic fibers. Leaky mode correction factors have been derived for elliptical core fibers [16].

Regardless of the appropriateness of a correction, the near field is a close approximation to the index profile for near parabolic fibers. Also, corrections mainly affect the 0.5a to 0.9a region and the apparent width of the pattern near the baseline is not affected. This is of importance in determining core diameter from near-field measurements.

For step index fibers, leaky modes are definitely significant and for short lengths the near field profile differs substantially from the index profile (see sect. 8.2).

It should be pointed out that the above comments apply only to multimode fibers with large numbers of modes. In fibers with single or few propagating modes, the near-field intensity distribution is given by the mode patterns themselves which can differ substantially from the index profile shape.

The near-field intensity distribution gives information on the spatial location of power in the fiber. Thus, one is measuring only the guiding regions of the fiber. What happens at the core cladding interface or in the cladding is not indicated.

2.2.2 Core Diameter

Core diameter is usually defined from the fiber refractive index profile. In one recommended definition, the core diameter is that diameter on the index profile where the refractive index of the core exceeds that of the cladding by k times the difference between the maximum refractive index in the core and the minimum index in the cladding, where k is a specified constant ($0 < k < 1$) [7]. Near-field measurements can be used to determine core diameter in some circumstances because of the close relationship between near field and refractive index profile. Leaky mode corrections, if they are even necessary for near parabolic index fibers, do not affect the measured width of the near-field pattern near the baseline. A core diameter measurement based on the full width at the 2 to 3 percent intensity points may be appropriate. A more serious uncertainty in determining core diameter results from the use of low index "barrier" layers between the core and cladding. How the near field is affected by such fluctuations near the cladding has not been established. Also, in graded index fibers, there is a loss of resolution near the core cladding boundary due to the decrease in local numerical aperture [17]. Some of these problems may be alleviated in a recently described "modified near-field" technique [18]. Despite some limitations, near-field measurements do indicate where power is spatially located in the fiber and, in some practical situations, this may be as important as the core diameter determined from an index profile.

2.3 Mode Volume Transfer Function--A Measurement Utilizing Both Far- and Near-Field Patterns

Holmes, et al., have introduced a concept describing the effect of propagation on spatial and angular intensity distributions in graded index fibers [4]. They define an "effective mode volume", EMV, based on far- and near-field intensity distributions. Specifically, the EMV at a given point along the fiber is the square of the product of the FWHM

(Full Width at Half Maximum) of the near field and the sine of the HWHM (Half Width at Half Maximum) of the far field.

EMV is related to the number of modes excited in the fiber. This can be intuitively seen when applied to the expression for the total number of guided modes, N, in a fully excited graded index fiber having a power law profile α [9].

$$N = \frac{\alpha\Delta}{2+\alpha} \left(\frac{2\pi n_1 a}{\lambda}\right)^2 \tag{5}$$

where a is the core radius, λ the wavelength, and other terms have been previously defined. After arranging terms,

$$N = \frac{\alpha}{2+\alpha} \left(\frac{2\pi^2}{\lambda^2}\right) [(NA) \cdot a]^2 \tag{6}$$

$$\approx \frac{\alpha}{2+\alpha} \left(\frac{2\pi^2}{\lambda^2}\right) \cdot \text{EMV} \tag{7}$$

Of interest is the EMV transfer characteristic for a fiber. This describes how various EMVs propagate in the fiber and is a plot of output EMV versus input EMV. By controlling launch spot and NA, various input EMVs can be generated. Input EMVs are determined from radiation patterns exiting a 2 m length at the input. The corresponding output EMVs are obtained from radiation patterns exiting the long length.

The EMV transfer characteristic gives information on mode coupling, differential mode attenuation, and quasi-steady state EMV. A fiber without mode coupling or differential mode attenuation appears as a 45° line on the transfer characteristic plot: i.e., the output EMV is equal to the input EMV.

A principle use of the EMV concept is in the prediction of concatenation. EMV transfer characteristics and attenuation versus EMV for all the fibers in the link allows one to predict accurately the concatenated attenuation for any input EMV [4].

3. DESCRIPTION OF FAR-FIELD MEASUREMENT SYSTEM

3.1 Source

The radiation source used with both far- and near-field systems is capable of producing independently variable spot sizes and launch numerical apertures, figure 3-1. Aperture 1, which controls launch spot size, is illuminated by either a strip filament lamp or a flat, close-coiled filament, quartz halogen lamp having an etched envelope. The lamp should have good spatial uniformity and, from this viewpoint, the strip lamp is preferred.

A broadband interference filter selects the nominal wavelength. Since these measurements are relatively insensitive to wavelength [19], a broadband filter with 80 nm linewidth gives improved signal-to-noise over narrowband filters. Angles of incidence on the filter are so small that angular dependent transmission effects are avoided.

The launch lens produces a demagnified image of aperture 1 on the fiber end; a demagnification ratio of 22 is typical and spot sizes down to 18 μm have been obtained. Aperture 2 controls the launch numerical aperture from a maximum of 0.36 to a minimum of 0.03.

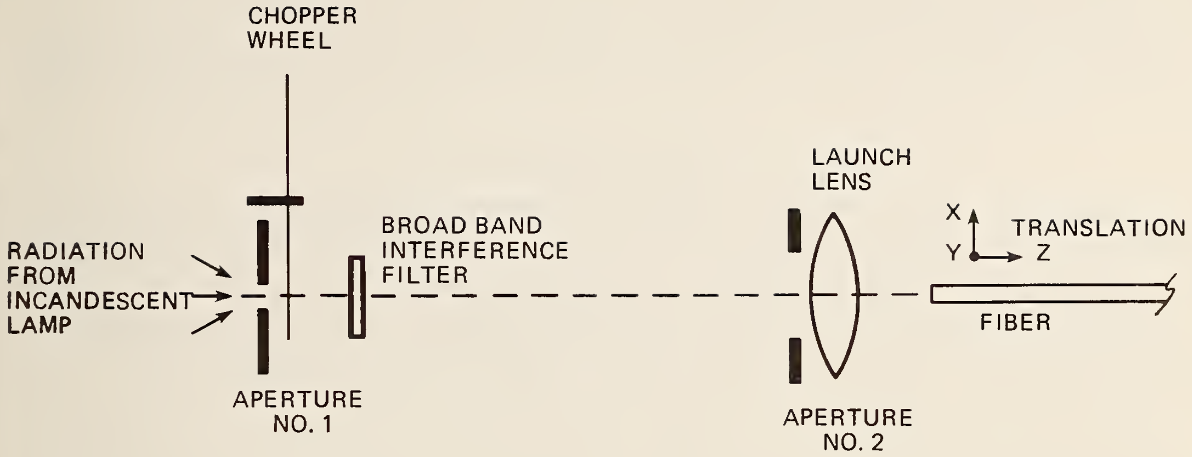

Figure 3-1. Launch optics used with far- and near-field systems.

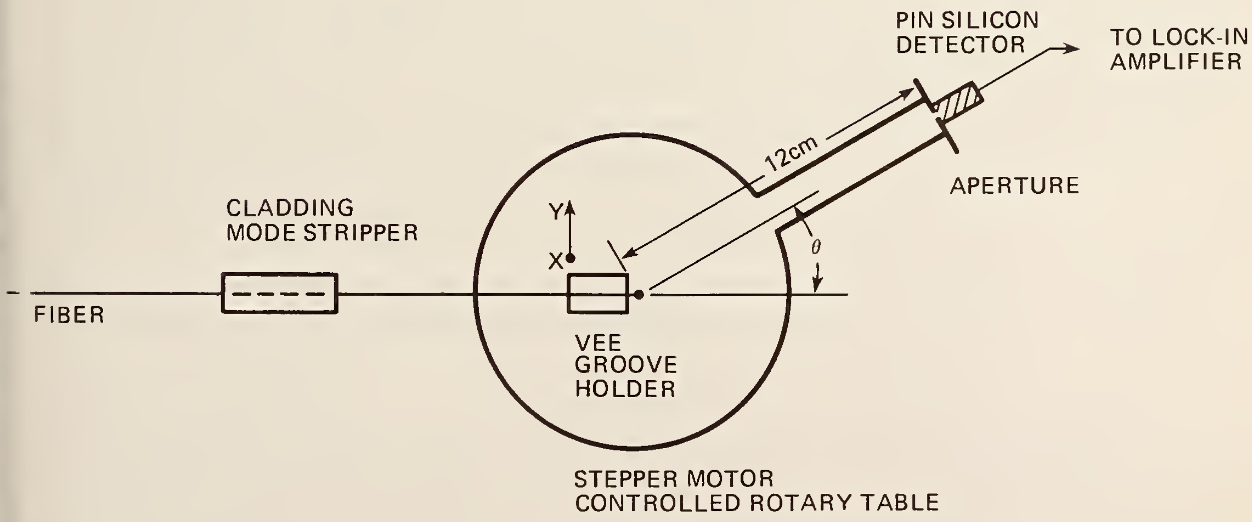

Figure 3-2. Far-field measurement system using a fixed fiber end and a rotating detector.

Overfilled launching conditions are used for most of the measurements, Table I. Therefore, additional optics to optically center the aperture image on the fiber end are not usually employed. Peak power transmitted through the fiber has been the alignment criterion when overfilled launching conditions are used.

A chopper wheel is located in the beam to modulate the light at 900 Hz. This provides a reference signal for narrowband, phase sensitive detection with a lock-in amplifier.

3.2 Detector

The far field may be scanned by a number of different techniques: (1) fixed fiber end, rotating detector, (2) fixed detector, rotating fiber end, (3) fixed fiber end, fixed detector, rotating mirror, and (4) fixed fiber end, detector array.

The system described in this Technical Note uses a fixed fiber end and a rotating detector, figure 3-2. This approach represents perhaps the simplest construction of available choices.

The fiber first passes through a cladding mode stripper consisting of two 10 cm long felt pads wetted with index matching fluid. Buffer coatings are removed from the fiber where it contacts the mode stripper. Near-field scans show this type of mode stripper effectively removes light from the cladding.

A vee groove positions the fiber so the end is coincident with the axis of rotation. Some measurements, especially near fields, are affected by the amount of force used to hold the fiber in the vee groove. These distortion effects are eliminated when a small, felt padded weight holds the fiber in the groove. Before making a measurement, the fiber end is visually inspected for flatness and perpendicularity. The vee groove position can be slightly adjusted by a two dimensional translation stage to assure that the detector scan passes through the maximum intensity part of the pattern.

Scanning is accomplished with a stepper motor controlled rotary table which swings the detector through a 12 cm radius arc. At this distance the far-field criteria is satisfied for core diameters of 100 μm or less. Angular motion (1/2 arc min. per step) is fine enough to give smooth far-field curves.

Detector aperture size is chosen with a trade-off between resolution and signal-to-noise ratio. Presently, a 0.8 mm diameter aperture is used giving a resolution of 0.38°.

Reducing aperture size to improve resolution, and hence accuracy, would not be important for most measurements which are relative comparisons (Table I). Radiation angle (NA) is the only far-field measurement which is absolute. A simple one-dimensional model based on a parabolic shaped far-field pattern with an NA of 0.2 predicts an error of 1.6 percent in the determination of radiation angle when the curve is acquired with 0.38° resolution. Measurement precision for determining radiation angle is in the range of 1 to 2 percent when a new output end is prepared and realigned (Sect. 4.1); therefore, a significant reduction in aperture size would not result in much improvement.

A silicon PIN diode operating in the photovoltaic mode is used as the detector [20]. This detector with an active area of 5.1 mm^2 has a built-in operational amplifier and is mounted directly behind the aperture. To improve signal-to-noise ratio, a time constant of

0.4 s is used on the lock-in amplifier. The scanning rate is chosen so a resolution element (0.38°) is scanned in approximately three time constants. At this rate a fiber far-field pattern is obtained in three to four minutes.

Data may be acquired by several methods. For curve fitting or numerical analysis, digital acquisition is necessary; however, for most applications, a good, wide paper strip chart recorder is adequate.

4. PERFORMANCE OF FAR-FIELD SYSTEM

4.1 Precision

Precision is a statement of measurement repeatability. It says nothing about a "systematic" error which is the offset of the average of a large number of measurements from the true value. Best precision is obtained when a measurement is repeated without disturbing any parameter. A typical example of this precision is given in figure 4-1. Here a far-field measurement was repeated seven times on graded index fiber A using overfilled launching conditions at a wavelength of 860 nm. Standard deviations for determining the full widths at the 80, 50, 20, 10, and 5 percent intensity points are shown. Error bars represent ± one standard deviation (2 standard deviations in length) and are given as a percentage of the full width at that particular point. A typical value is in the 0.5 percent range. It should be noted that the width of an ink line is approximately 0.3 percent of the curve FWHM and therefore represents a limitation in determining actual precision. The main conclusion drawn from figure 4-1 is that the system has no appreciable dc drift problems.

For many measurements, the above precision is not applicable. In practice, new ends must be prepared and the system aligned. To determine this precision, far-field measurements were repeated seven times, for each measurement a new output end was prepared and the system slightly realigned to the maximum intensity point. Three different fibers representing two different manufacturers were measured, figures 4-2 and 4-3 [21]. Standard deviations for graded index fiber B (not shown) were about 1 percent on lower parts of the curve. For graded index fiber A the corresponding values are a little higher--in the 1 to 2 percent range. Fiber C, with a step index, has a much flatter top in general agreement with theory [22]. Here the precision is also in the 1 to 2 percent range. From these tests, a precision of 1 to 2 percent is indicated for a radiation angle measurement.

4.2 Accuracy

Accuracy is determined by the absolute value of the angular calibration factor, angular resolution, and system linearity. The angular calibration factor was determined by reflecting a low divergence He-Ne laser beam off a mirror attached to the rotary table and onto the laboratory wall. The table was rotated through 360° and the beam returned, within the nearest step, to the original position. This procedure determines the angular rotation per step more accurately than is practically needed.

As previously mentioned, the finite angular resolution introduces an error when determining the radiation angle. This error is estimated to be less than 1.6 percent.

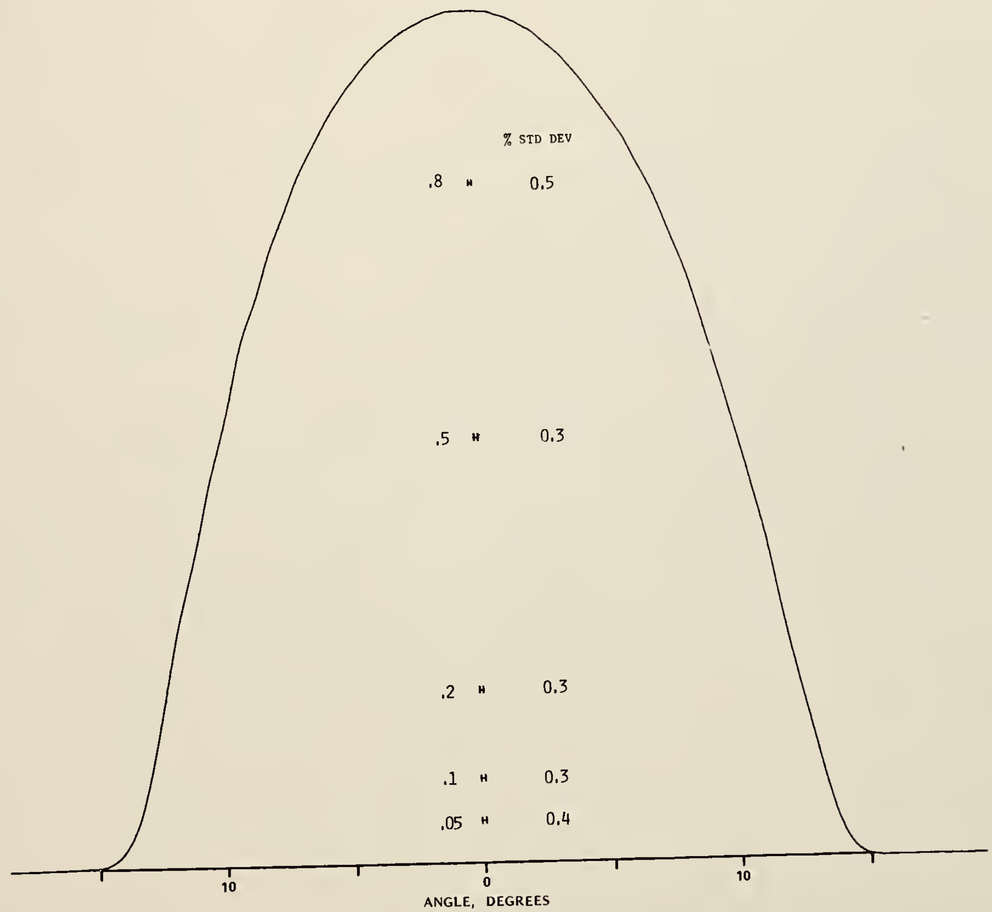

Figure 4-1. Far-field measurement precision when no parameters are changed. Fiber A, graded index, 1.1 km length, 5 dB/km, 0.23 NA, 860 nm; ± one standard deviation indicated along ordinate at 0.8, 0.5, 0.2, 0.1, and 0.05 of maximum as a percentage of full angular width at that point.

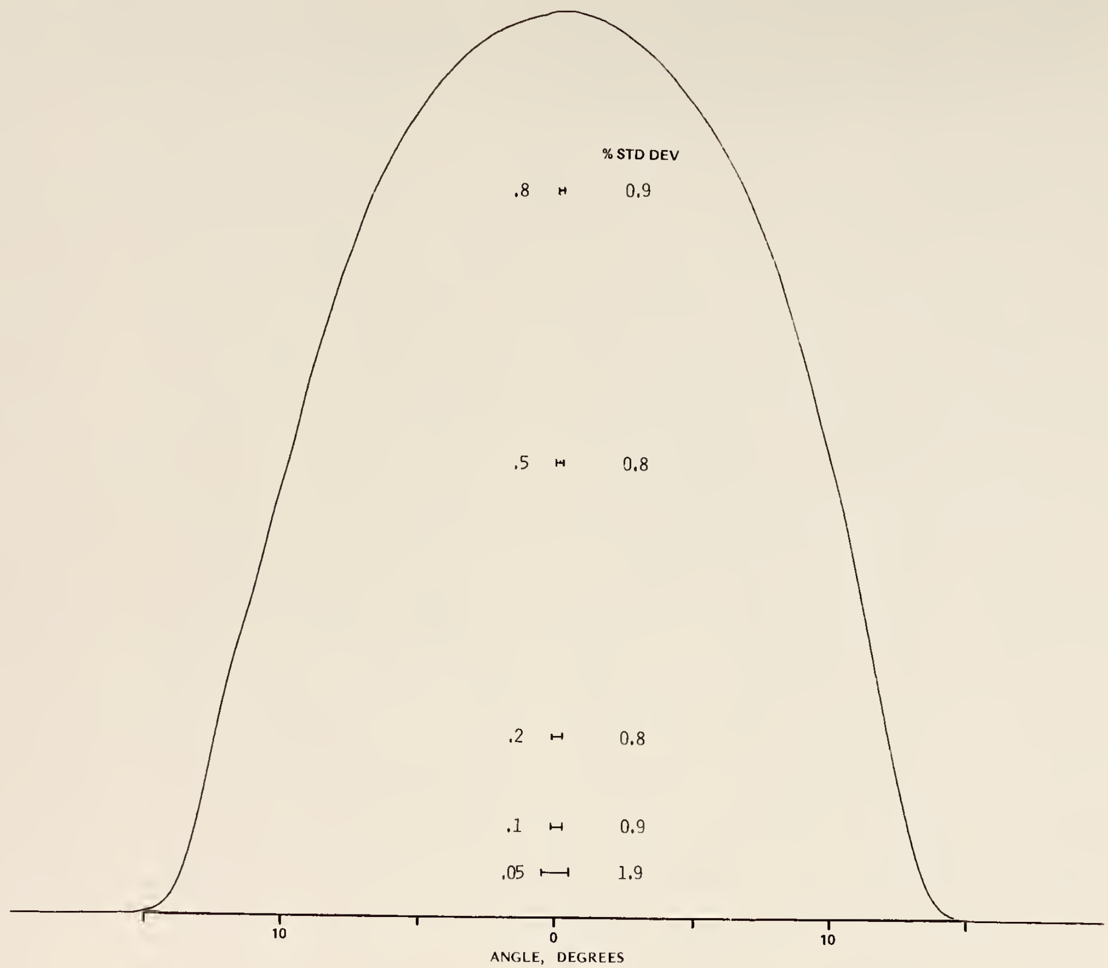

Figure 4-2. Far-field measurement precision with recleaved output end and realignment for each measurement. Graded index fiber A; ± one standard deviation indicated along ordinate at 0.8, 0.5, 0.2, 0.1 and 0.05 of maximum.

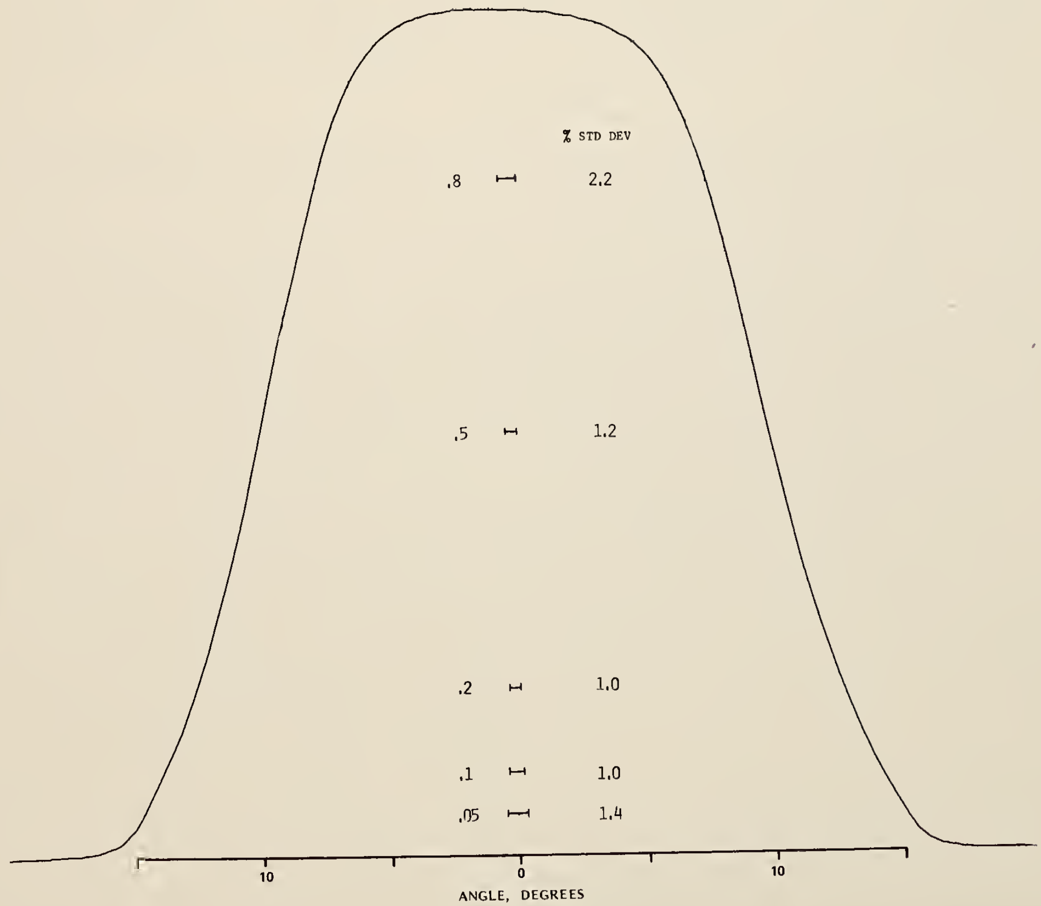

Figure 4-3. Far-field measurement precision with recleaved output end and realignment for each measurement. Fiber C, step index, 1.2 km length, 6 dB/km, 860 nm; ± one standard deviation indicated along ordinate at 0.8, 0.5, 0.2, 0.1, and 0.05 of maximum.

Detector non-linearity could affect the shape of the measured pattern. A calibrated neutral density filter was used to confirm detector linearity up to the highest power levels used with the system.

4.3 Dynamic Range

Signal-to-noise ratio was determined by attenuating the source until the noise level was observed. Figure 4-4(A) shows the far field from a fiber having a loss of 5 dB when excited with overfilled launch conditions. In figure 4-4(B), the source is attenuated by approximately 17 dB to display the noise level. Also shown is the noise level on the baseline and at the peak value; in both cases the noise is about 4 μV peak-to-peak. Signal-to-noise ratio for a short length of fiber, having negligible attenuation, is 34 dB at 860 nm using an 80 nm bandpass interference filter, overfilled launching conditions, and a time constant of 0.4 s on the lock-in amplifier. In figure 4-4(B) the signal-to-noise ratio is 12 dB and represents the lowest level for making a reasonable measurement. Based on this criteria, the system has a dynamic range of 22 dB. There are measurements, especially with very restricted launching conditions, where more signal-to-noise would be desirable. The easiest way to increase signal is to increase source linewidth. For some measurements this may be acceptable. An additional 7 dB improvement in signal can be obtained by replacing the broadband interference filter with a long pass filter having a cut-on wavelength of 0.78 μm. In this case the long wavelength cutoff, 1.1 μm, is determined by the spectral response of the silicon detector.

5. TYPICAL RESULTS FROM FAR-FIELD MEASUREMENTS

5.1 Radiation Angle (Numerical Aperture)

Radiation angle was determined for a number of commercially available multimode fibers. Measurement precision was consistent with the results of section 4.1. Figure 5-1(A) is a typical result from a graded index fiber with a rather low NA of 0.16; while figure 5-1(B) shows a fiber with a rather high NA of 0.23. Results of figure 5-1 were obtained using overfilled launching conditions on a 2 m length of fiber. In almost all cases, far-field patterns from commercial graded index fibers have been smooth, bell shaped, and exhibit a single central maximum.

5.2 Attenuation with Restricted Launch via a Mode Filter

Radiation pattern measurements on both long (1 km or more) and short (2 m) lengths of the same fiber are necessary to qualify mode filters for restricted launch attenuation measurements. A successful mode filter produces an output radiation angle from a 2 m length equivalent to the output radiation angle from the full test length excited by overfilled launching conditions. Restrictions in radiation angle, due to fiber propagation, are a function of differential mode attenuation and mode coupling. For many typical graded index fibers, the radiation angle from an overfilled launch restricts by 4 to 8 percent after a kilometer of propagation.

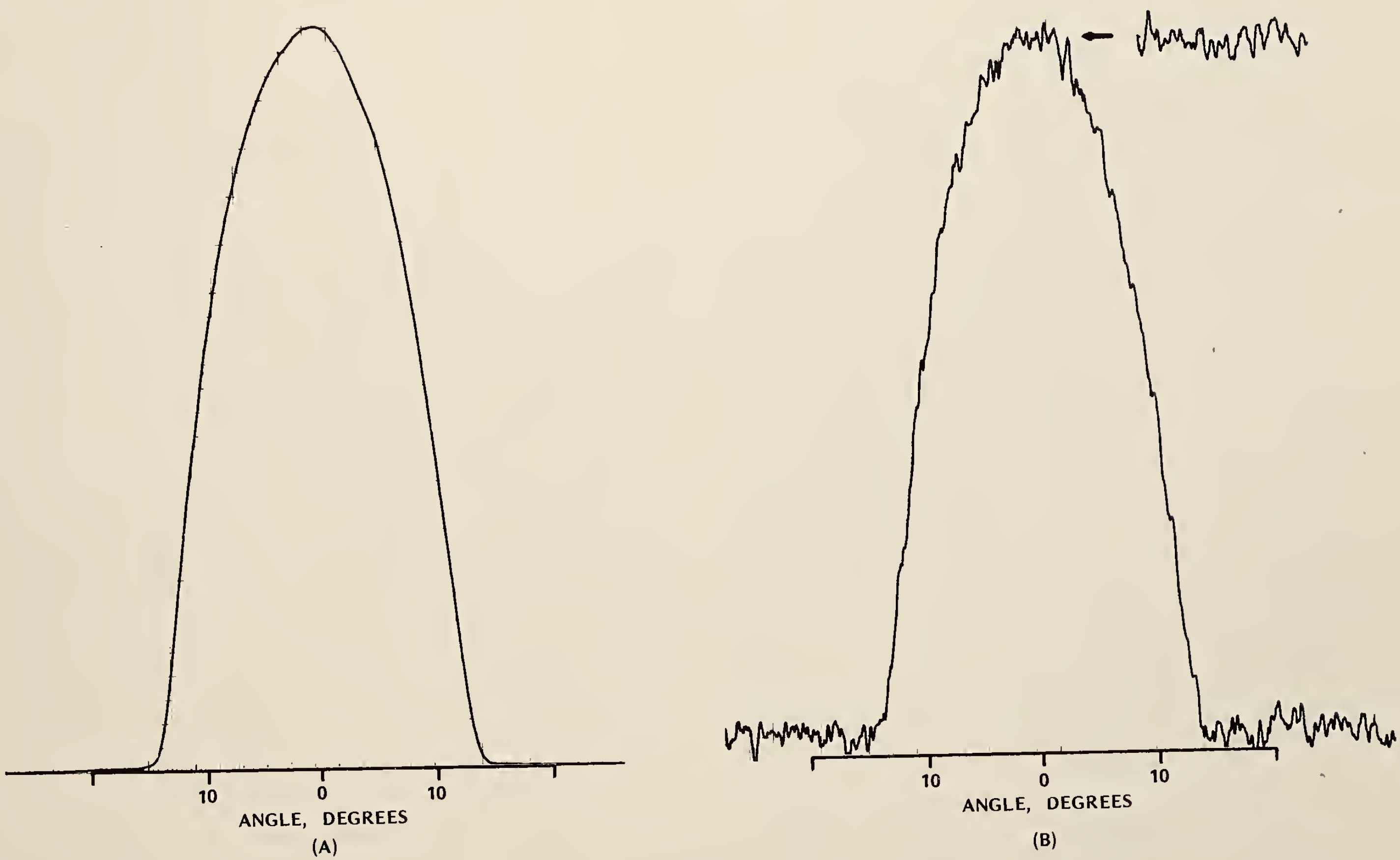

Figure 4-4. (A) Far field from graded index fiber having a loss of 5 dB: (B) same as (A) but with source attenuated by 17 dB, signal to noise of (B) is 12 dB.

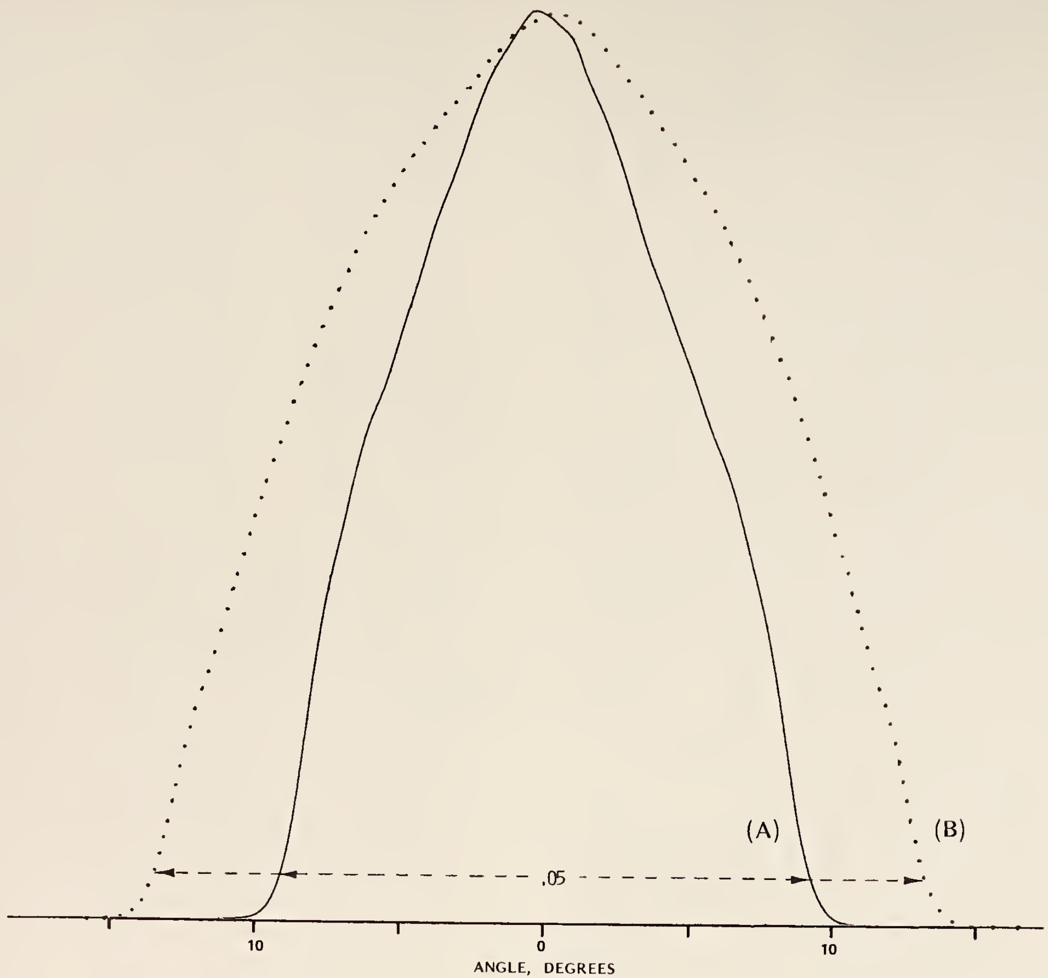

Figure 5-1. Examples of graded index fibers with high and low radiation angles (5 percent intensity width). NA's of 0.16 and 0.23 are obtained from curves (A) and (B) respectively.

One mode filter possibility is a series of serpentine, macroscopic bends, figure 5-2. This geometry in a step index fiber has been previously used as a mode-scrambler for bandwidth measurements [23] [24]. The specific geometry used here consists of eleven, 9 mm diameter nylon posts--six fixed and five moveable. A fiber is placed in the mode filter and the moveable posts are translated to produce sinusoidal bends having a period of 22 mm with variable amplitude. Maximum far-field restrictions are obtained when the posts are evenly aligned (9 mm peak-to-peak amplitude).

The effect of this mode filter on the far-field pattern from a short length of graded index fiber is shown in figure 5-3. The solid curve was obtained without the mode filter using overfilled launching conditions to the 2 m length. The dotted curve is the same but with the mode filter set to maximum amplitude. A restriction of 16 percent in radiation angle is achieved at maximum amplitude. This particular fiber, when excited by overfilled launching conditions, exhibits a 6 percent restriction in radiation angle after 0.9 km of propagation. Thus, the serpentine mode filter in this case would be more than adequate to achieve the necessary restriction (9 percent) for an attenuation measurement.

It should be emphasized that mode filters affect different fibers in different ways. The exact nature of the mode reduction is a function of: mode filter, buffer coating, cladding diameter, core diameter, numerical aperture, etc. Fibers have been found where the serpentine mode filter has produced significantly different results than figure 5-3. It is therefore necessary to "qualify" a mode filter for the particular class of fibers being measured.

5.3 Symmetry of Radiation Patterns

In general, far-field measurements on single core fibers give smooth, symmetric, bell shaped curves having a single maximum. Fine structure from the core would be diffracted into relatively large angles. For example, a plane wave illuminating a circular aperture of diameter d has a diffraction angle of 1.22 λ/d. This is 1.4° when applied to a 50 μm diameter core at a wavelength of 1 μm.

Pattern symmetry is indicated in figure 5-4. Here far-field patterns are folded about a vertical axis passing through the midpoint of the width at half maximum. These examples were selected from measurements on a large number of commercial fibers and are typical of good and poor symmetries. Even in the poor case, the symmetry is fairly good.

5.4 Mode Dependance of OH^- Absorption

The OH^- radical causes spectrally localized absorption in optical fibers. One of the stronger lines occurs near 950 nm. Previous backscatter measurements show that OH^- is not necessarily distributed uniformly along the fiber length [25]. This section describes far-field measurements to qualitatively determine the mode dependence of OH^- absorption in a particular fiber.

For these measurements, a 0.9 km fiber was chosen with a large OH^- absorption peak and little mode coupling. Spectral attenuation measurements indicate a loss of 5 dB/km at 850 nm which increases to 40 dB/km at 950 nm. By analyzing far-field patterns at 850 nm

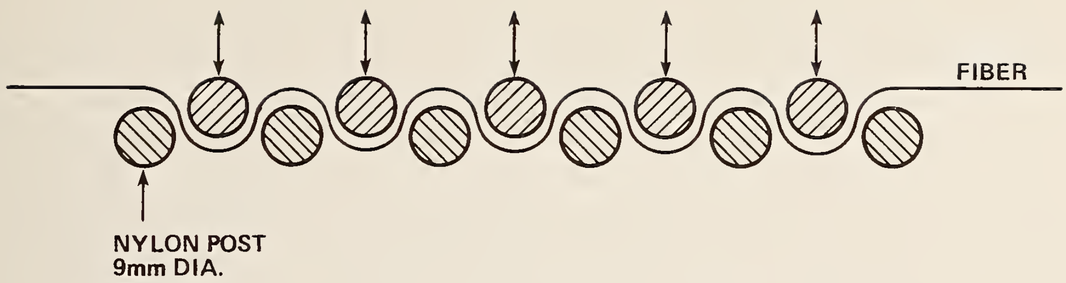

Figure 5-2. One type of mode filter consisting of a series of serpentine, macroscopic bends. Moveable posts can be translated into alignment with fixed adjacent posts.

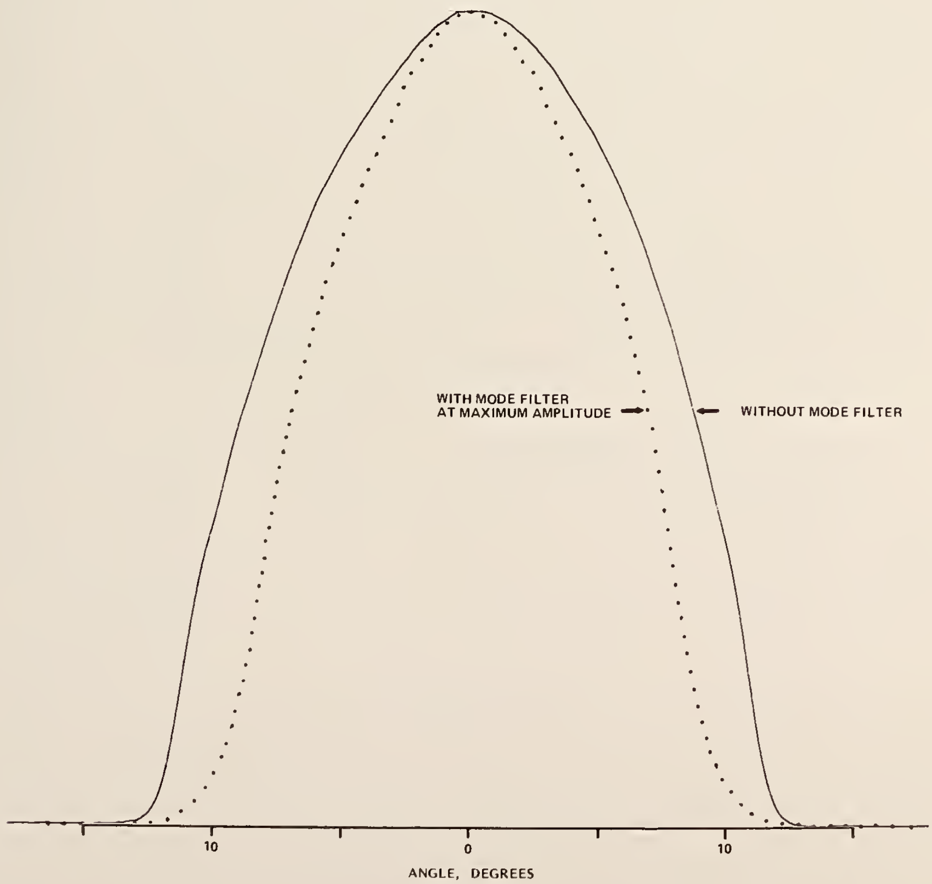

Figure 5-3. Effect of mode filter on 2 m length of graded index fiber. Solid curve is without mode filter, dotted curve is with mode filter set at maximum amplitude.

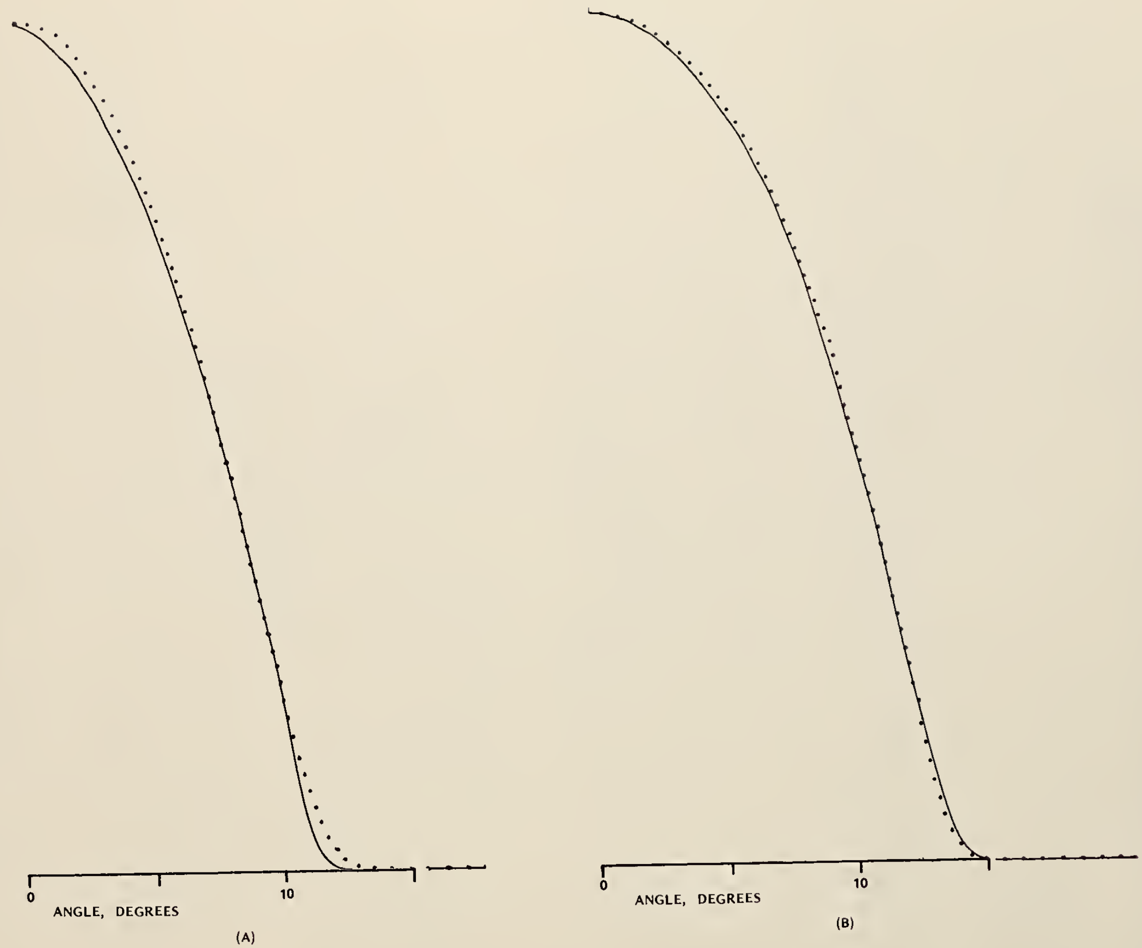

Figure 5-4. Typical symmetry of far-field patterns from graded index fibers. Left part of pattern (dotted line) is folded about a vertical axis through mid-point of half maximum width to compare with right part of pattern (solid line). Far-field (B) exhibits better symmetry than far-field (A).

from overfilled and restricted mode volume launches, this fiber was found to have little mode coupling.

Qualitatively, if more OH^- were located near the core-cladding interface, higher order (large radius-large angle) modes would be attenuated more and a narrower pattern would result at the output from an overfilled input; the converse would be true if the OH^- were concentrated near the axis.

Figure 5-5 is the superposition of normalized far-field patterns at 857 nm and 957 nm using overfilled launching conditions and 70 nm bandpass filters. Precision in determining these differences should be quite good since only interference filters were changed between the two measurements. As shown, the presence of OH^- absorption at 957 nm does little to alter the shape from the pattern at 857 nm where no OH^- absorption is present. Therefore, the OH^- in this fiber appears to be uniformly distributed with a slight indication of more OH^- near the axis (957 nm curve is wider). The distribution of OH^- would depend upon the preform fabrication process so the above results apply only to the particular fiber.

6. DESCRIPTION OF NEAR-FIELD MEASUREMENT SYSTEM

The near-field system produces a magnified image of the fiber end face. A single microscope objective gives a magnification of about 50, figure 6-1. By scanning a detector across a diameter of the image, the near-field intensity distribution is obtained. In figure 6-1, the detector aperture is located at a fixed distance from the objective so the magnification ratio remains constant independent of other system adjustments.

The detector is an apertured silicon PIN photodiode identical to the one used with the far-field system. This detector is scanned across the image, which is nominally a few mm in diameter, by a stepper motor controlled translation stage having a movement of 0.4 μm per step. The detector aperture size, 80 μm diameter, was chosen to be consistent with theoretical resolution limits. A smaller size does not improve resolution but results in lower signal-to-noise ratio. An 80 μm aperture gives a resolution of 1.5 μm when referenced to the fiber endface.

Care should be used in selection of the fiber holder, which is positioned just after the cladding mode stripper. The present system uses a vee groove with a small, felt padded weight to hold the fiber in the groove. If the fiber is held with too much force, stress will distort the near-field intensity distribution and scatter light into the cladding. The vee groove is mounted on an xyz translation stage so the image can be brought into focus on the detector aperture.

Alignment is accomplished using the movable mirror and eyepiece shown in figure 6-1. First, a fiber is imaged in the system at the measurement wavelength (typically 850 nm); good sensitivity is obtained by imaging the on-axis index dip. Then, using deep red visible light, the movable mirror is positioned to illuminate the eyepiece. The eyepiece is translated until the image appears in sharp focus. Now, if a fiber end is brought into focus using the eyepiece, it will be in proper focus at the detector aperture when the mirror is moved out of position. This method of alignment was checked using a number of fibers.

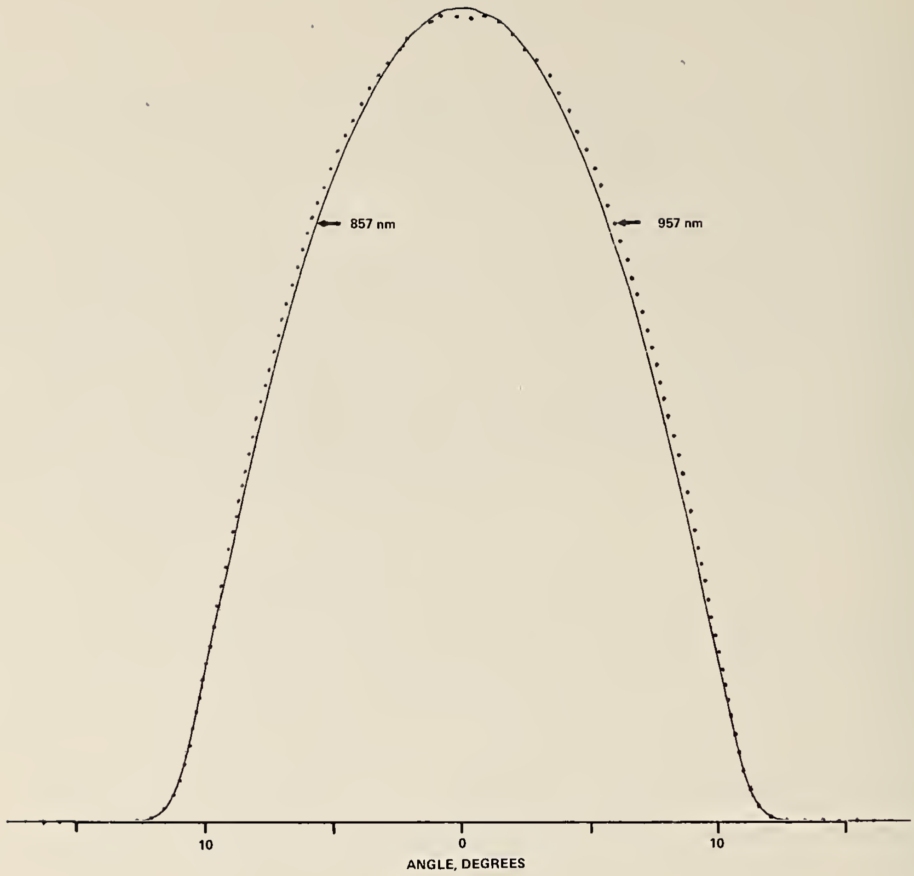

Figure 5-5. Experiment to qualitatively determine mode dependence of OH^- absorption. Little mode dependence is indicated for this particular fiber.

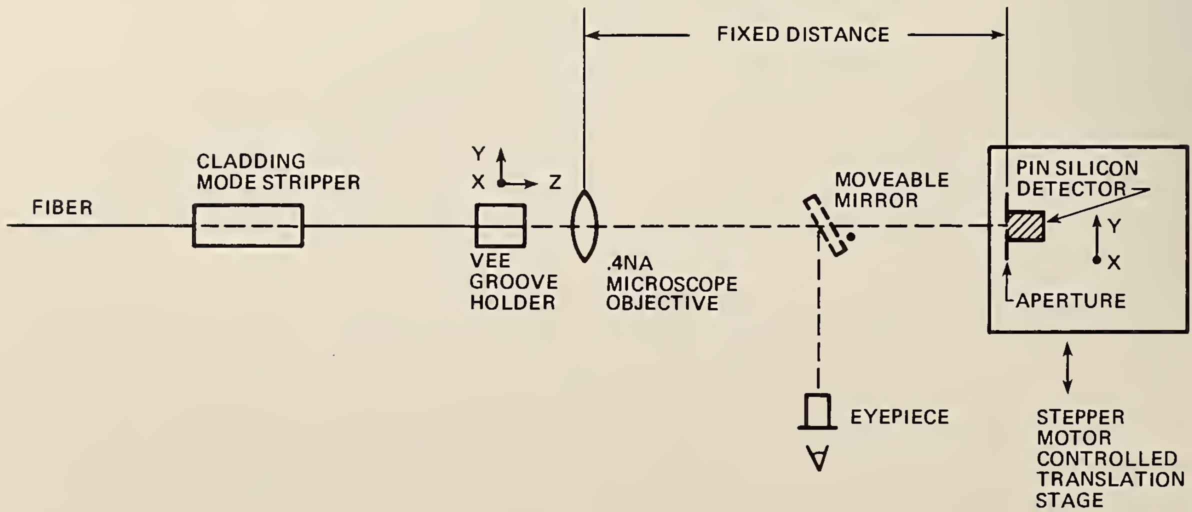

Figure 6-1. Near-field measurement system based on a radial scan of a magnified near-field image.

Fibers were first aligned visibly with the eyepiece; no further improvement in the focus of index dips could be obtained at the detector using 850 nm light.

The source used with the near-field system was previously described in section 3.1. Scan rate and lock-in amplifier time constant were chosen with a trade-off between mechanical drift and signal-to-noise ratio. Presently, the system scans a 50 μm core in 5 minutes with a detection time constant of 0.13 s. These issues are addressed more fully in sections 7.2 and 7.3.

7. PERFORMANCE OF NEAR-FIELD SYSTEM

7.1 Precision

Best precision is obtained when the measurement is repeated without disturbing any parameter except refocus. Figure 7-1 shows the results of four repeated measurements on a 1.1 km length of graded index fiber D. The standard deviations for determining the full widths at the 80, 50, 20, 10, and 3 percent intensity points are indicated along the ordinate in the figure. A typical value is in the 0.3 percent range for the lower part of the curve. It should be noted that the width of an ink line is approximately 0.2 percent of the FWHM and therefore represents a limitation in determining actual precision. The main conclusion from figure 7-1 is that the system has no appreciable dc drift during a 10 minute period.

In practice, new ends must be prepared and the system refocused. To determine this precision, near-field measurements were repeated four times with new end preparation and alignment for each measurement. Three fibers, two graded and one step, D, E, and C, were used for this test; results on E and C are given in figures 7-2, and 7-3. For fibers E and C, standard deviations for determining full-widths on the lower parts of the curves range from 0.8 to 1 percent. For fiber D (not shown), the corresponding values are slightly higher, 1 to 2 percent. This precision data contains effects of core ellipticity since fibers were remeasured without regard to angular orientation. A precision of about 1.5 percent would apply to a core diameter measurement based on a determination of the near-field full width close to the baseline on a short length of fiber.

7.2 Resolution and Accuracy

When all light emitted by the fiber is collected by the objective, the near-field resolution is determined by fiber numerical aperture. This is a consequence of the expression for the resolution, Y, of a microscope objective with

$$Y \sim \frac{0.6\lambda}{NA} . \tag{8}$$

Where λ is the wavelength and NA refers to the collected numerical aperture [26]. At a λ of 0.85 μm and an NA of 0.2, Y is 2.6 μm.

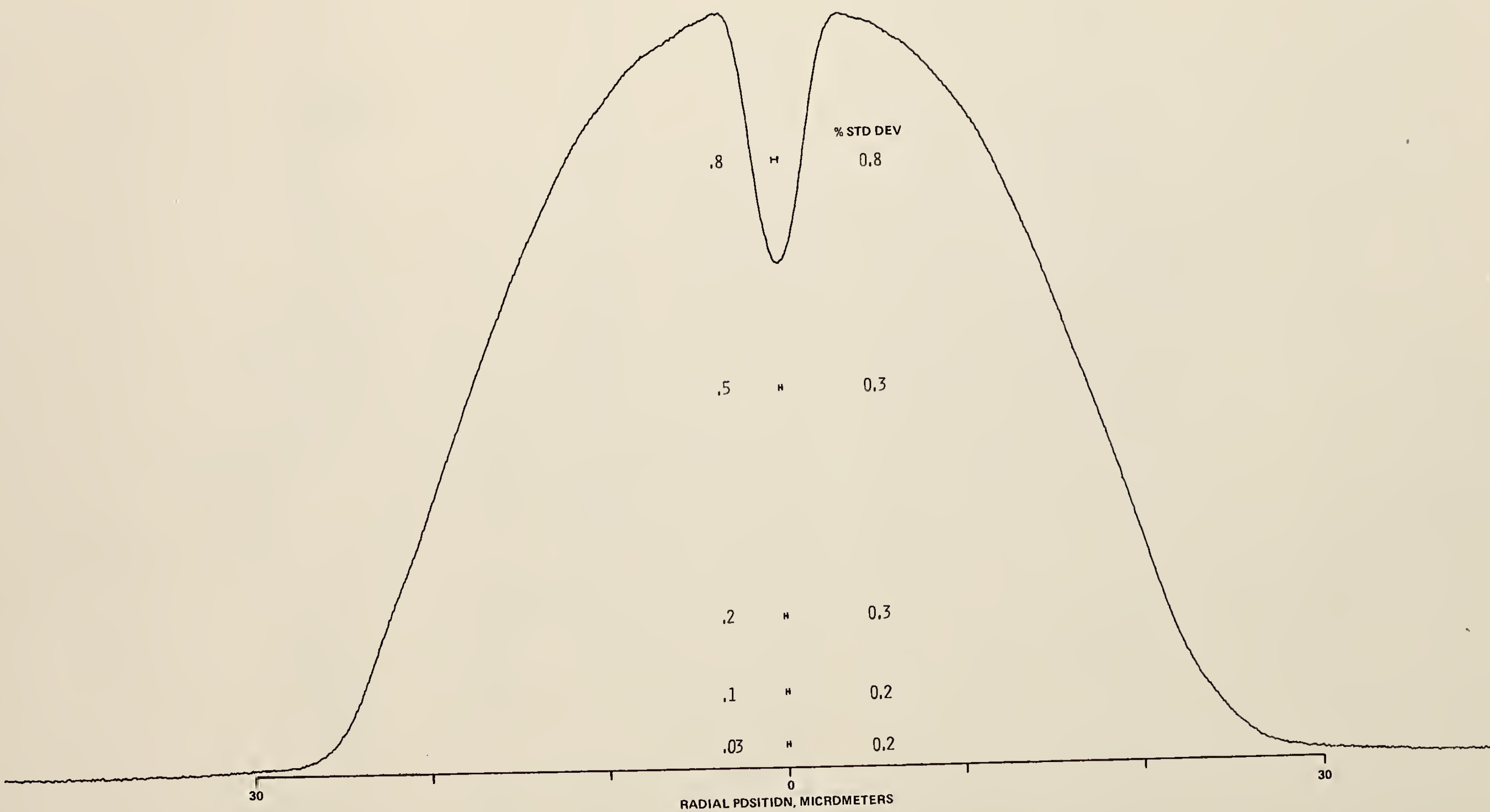

Figure 7-1. Near-field measurement precision when no parameters are changed. Fiber D, graded index, 1.1 km length, 6 dB/km, 0.23 NA, 860 nm; ± one standard deviation indicated along ordinate at 0.8, 0.5, 0.2, 0.1 and 0.03 of maximum as a percentage of full width at that point.

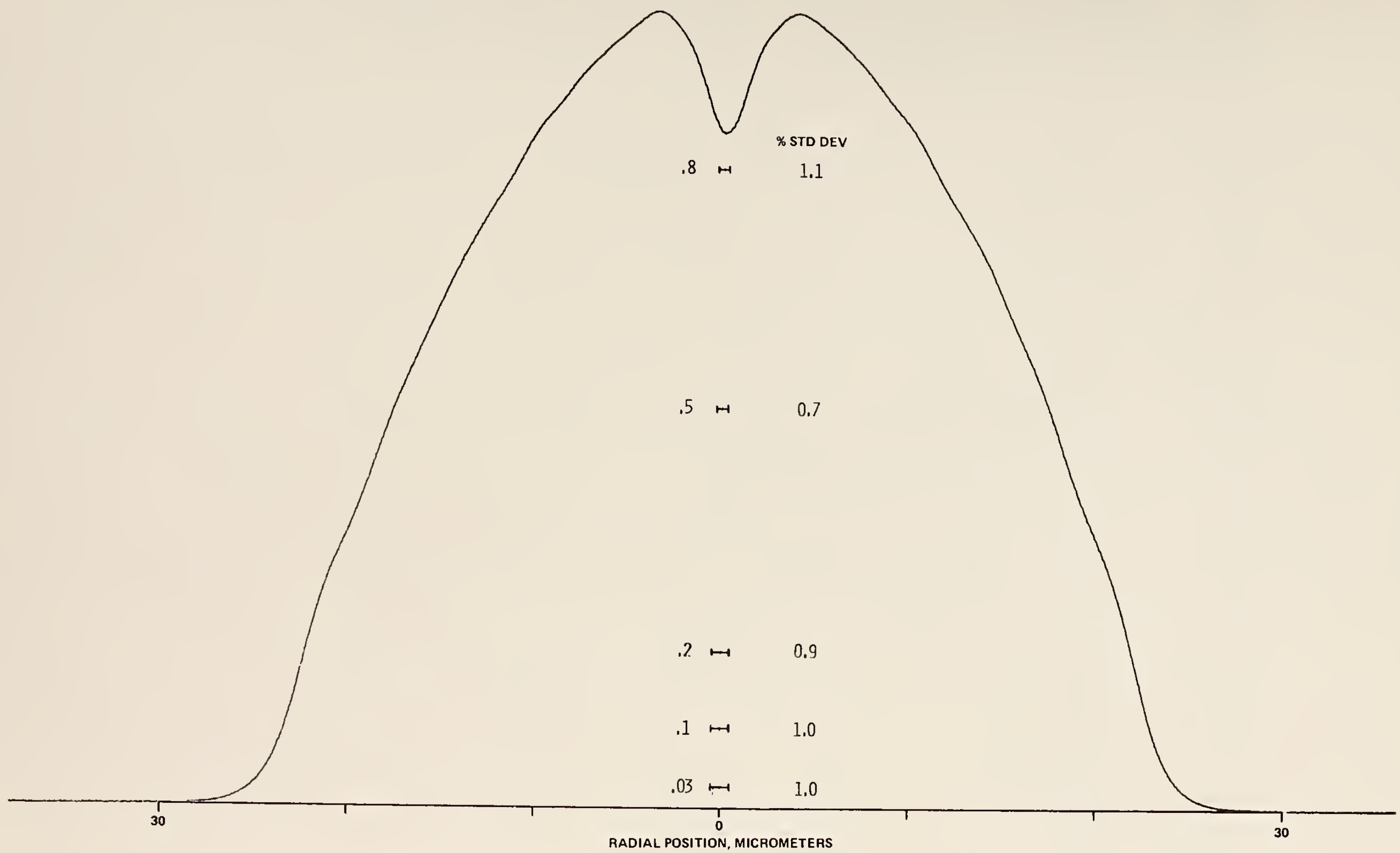

Figure 7-2. Near-field measurement precision with recleaved output end and realignment for each measurement. Fiber E, graded index, 5 m length, 0.20 NA, 860 nm; ± one standard deviation indicated along ordinate at 0.8, 0.5, 0.2, 0.1 and 0.03 of maximum.

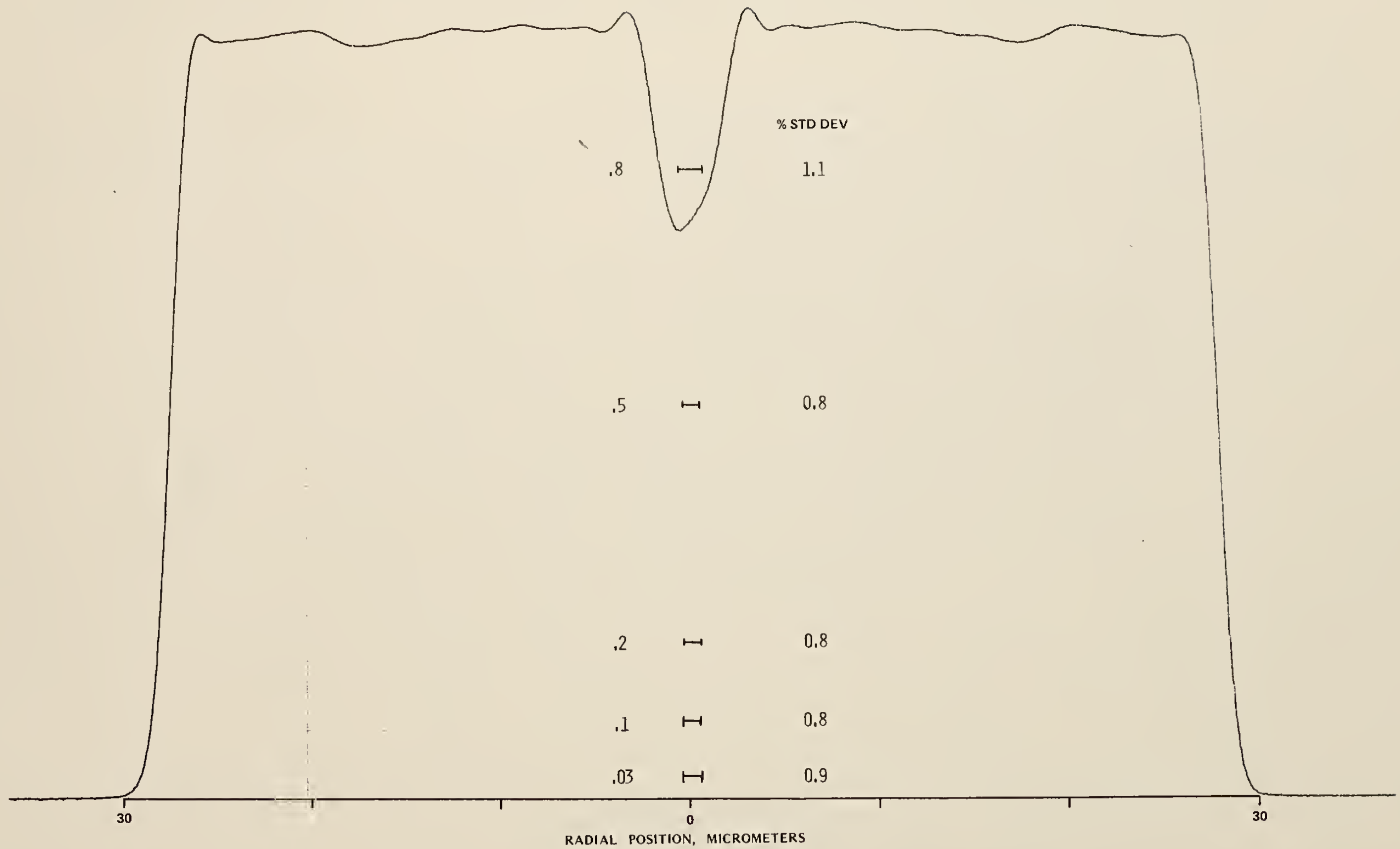

Figure 7-3. Near-field measurement precision with recleaved output end and realignment for each measurement. Fiber C, step index, 1.2 km length, 6 dB/km, 860 nm: ± one standard deviation indicated along ordinate at 0.8, 0.5, 0.2, 0.1 and 0.03 of maximum.

In a more detailed treatment where mode amplitudes are summed, Adams et al., show that near-field resolution is related to the number of propagating modes and, for a near parabolic fiber is approximately 2 a/V, where V is the normalized frequency [27]. V is given by [9] as

$$V = \frac{2\pi}{\lambda} a\ (NA)\ . \tag{9}$$

Thus, the resolution becomes $\lambda/\pi NA$, which is about a factor of two less than eq (8). Theoretical limits therefore are approximately 2 μm for a 0.2 NA graded index fiber at a wavelength of 0.85 μm.

Experimentally, upper limits to resolution were obtained by observing abrupt features in near-field patterns. This includes index dips and core-cladding boundaries. Upper limits are obtained since the actual shapes of the features are unknown. Figure 7-4(A) shows the narrowest index dip, 2.5 μm FWHM, observed with the system. Figure 7-4(B) is a 1.9 μm 10 to 90 percent edge response to a core cladding boundary in a step index fiber after 1.1 km of propagation (leaky modes have died out). Both of these cases suggest a resolution near 2 μm consistent with theoretical expectations.

The scanned dimension must be calibrated to make an absolute measurement. At present, this is accomplished with a microscope stage micrometer having rulings every 10 μm. These rulings are illuminated from behind the stage substrate with light, at the actual measurement wavelength, from a large core, large NA fiber. A typical calibration scan is shown in figure 7-5. Here the imaged rulings transmit more light than the background and appear as a series of peaks separated by 10 μm. A close inspection of figure 7-5 shows the peaks are not exactly evenly spaced. We believe this is caused by uneven illumination across the widths of the rulings. Such behavior can be observed by eye using visible light. Presently a centrally located pair of lines spaced by 150 μm is used to determine the calibration factor. In this way, the uncertainty in calibration due to uneven ruling illumination is reduced so resolution and stage micrometer accuracy become the limiting factors.

Preliminary results have been obtained to verify the calibration of commercial stage micrometers. In this measurement the spacings between rulings are compared to transmission fringes from a Fabry Perot interferometer, figure 7-6. Rulings which have higher transmission are located by a HeNe laser beam focused to 2 μm. A motorized differential micrometer drives the stage and translation is measured by counting fringes. With an HeNe laser, transmission fringes occur every $\lambda/2$ or 0.3164 μm. The Fabry Perot free spectral range is large enough so cavity modes from a common HeNe alignment laser are not observed. Figure 7-7 shows a typical result; in this case ruling centers are separated by 316 fringes (nearest integer fringe) or 99.98 μm. The average of 9 measurements over various ruling pairs was 100.4 μm with a standard deviation of 0.5 μm--in reasonable agreement with the stated spacing of 100 μm. Further improvement would be expected by focusing the HeNe beam to a smaller spot and using a stage micrometer with sub-μm ruling widths.

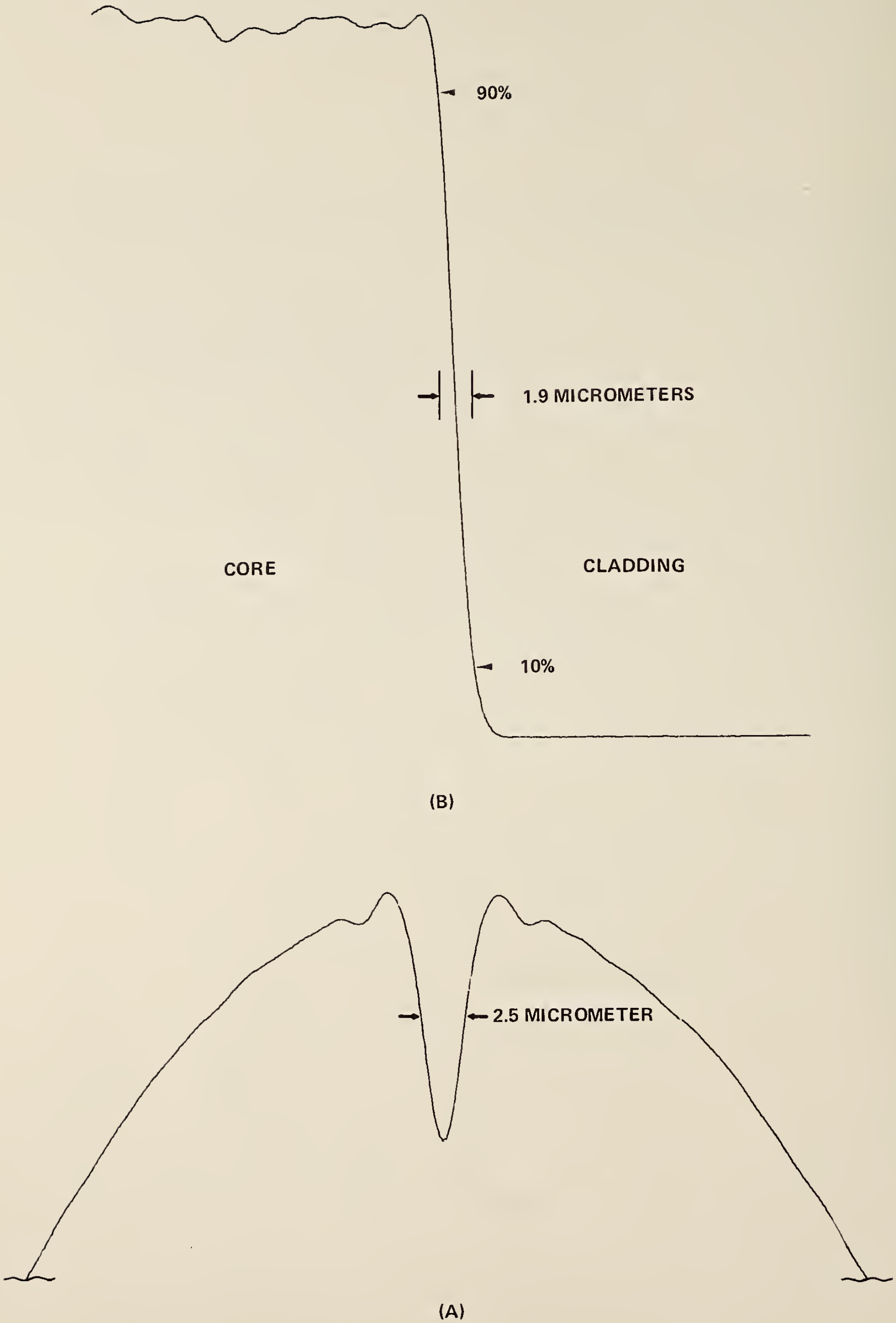

Figure 7-4. Experimental upper limits to near-field resolution at 860 nm. (A) narrowest on-axis index dip observed, (B) 10 to 90 percent edge response to core cladding boundary on Fiber C.

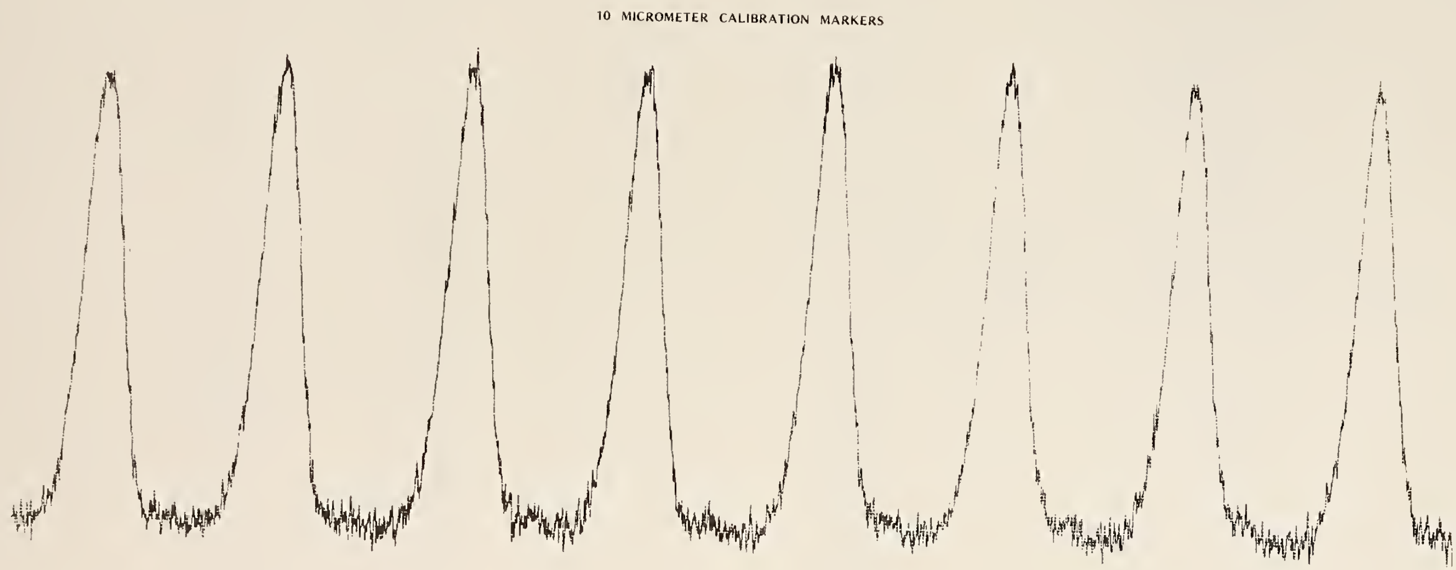

Figure 7-5. Calibration peaks for the near-field system obtained from imaging a microscope stage micrometer.

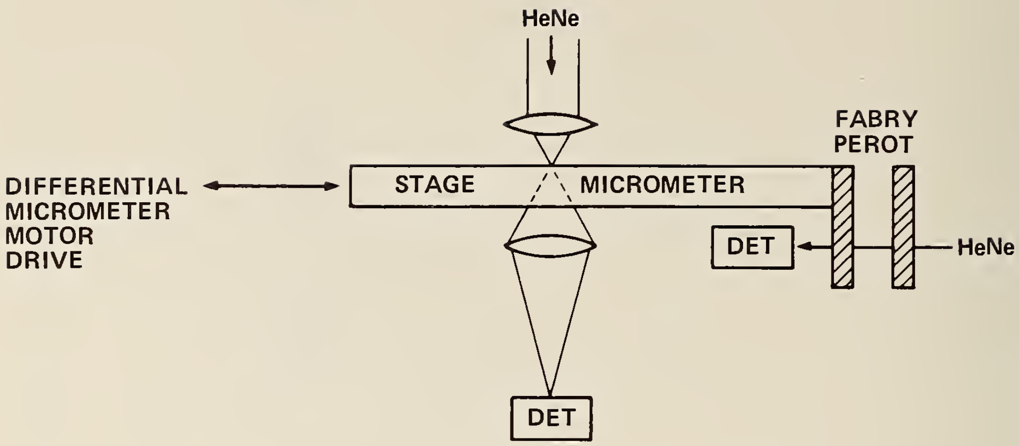

Figure 7-6. Apparatus to reference stage micrometer ruling spacings to transmission fringes from a Fabry Perot interferometer.

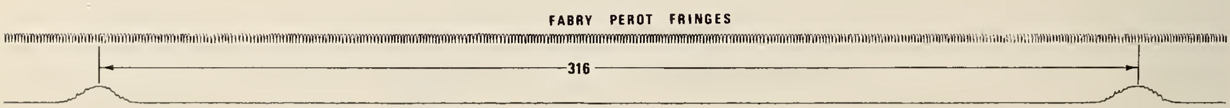

Figure 7-7. A comparison of ruling spacing (100 μm nominal) to counted fringes (316 x 0.3164 μm = 99.98 μm).

7.3 Dynamic Range

The source was attenuated until noise was observed on the near-field pattern from a 2 m length of graded index fiber, figure 7-8. In this instance the source (850 nm wavelength, 80 nm linewidth) was attenuated by 22 dB, thus indicating a signal-to-noise ratio of 39 dB with an unattenuated source. Figure 7-8 with a signal-to-noise ratio of 17 dB represents the lowest signal-to-noise ratio for extracting useful information; thus, fiber losses of up to 22 dB can be accomodated by the system.

Further improvements in signal-to-noise ratio could be achieved by increased source linewidth or lock-in amplifier time constant. Figure 7-8 was scanned in about 10 minutes, substantially longer scan times would cause the system to drift out of focus. Mechanical drift is minimized by mounting all components securely to a 5 cm thick aluminum plate. With a 10 minute total scan time, the lock-in amplifier time constant could be increased about a factor of five over figure 7-8 to pick up an additional 4 dB in signal-to-noise ratio.

8. TYPICAL RESULTS FROM NEAR-FIELD MEASUREMENTS

8.1 Cladding Light

Signal-to-noise ratio is sufficient to observe light scattered into the cladding due to stress on the fiber, incomplete mode stripping, etc. Figure 8-1 shows a scan over an entire fiber diameter to detect light in the cladding; the cladding-air boundary is clearly shown. Cladding light can be measured with a signal-to-noise ratio consistent with section 7.3.

8.2 Step Index Fibers

Several examples have already been given in this Technical Note of near fields from graded index fibers. In contrast, short step index fibers are greatly affected by the presence of leaky modes. Figure 8-2 is the superposition of near-field patterns from the same step index fiber at a length of 1 m and 1.1 km. In 1.1 km, the leaky modes have been attenuated so the near field closely resembles the index profile of a step fiber.

8.3 Symmetry of Radiation Patterns

From the very nature of the preform fabrication process, fibers should exhibit good symmetry across a diameter. However, at times, cores can be out of round and not necessarily concentric with the outside cladding boundary. Figure 8-3 shows typical near-field measurements from fibers. To illustrate radial symmetry the patterns have been folded about a vertical axis passing through the midpoint of the width at half maximum. As shown, the deviations are slight and lines nearly overlap. The more asymmetric behavior that has been observed has usually occurred within the index dip on-axis.

8.4 Index Dip Pathologies

Fibers made by chemical vapor deposition processes generally show an on-axis dip in the index profile. This happens when the preform is either consolidated or collapsed and dopants evaporate out of the axial region [9]. Attempts have been made to compensate this process, giving rise to index peaks in cases of overcompensation [28]. This section is

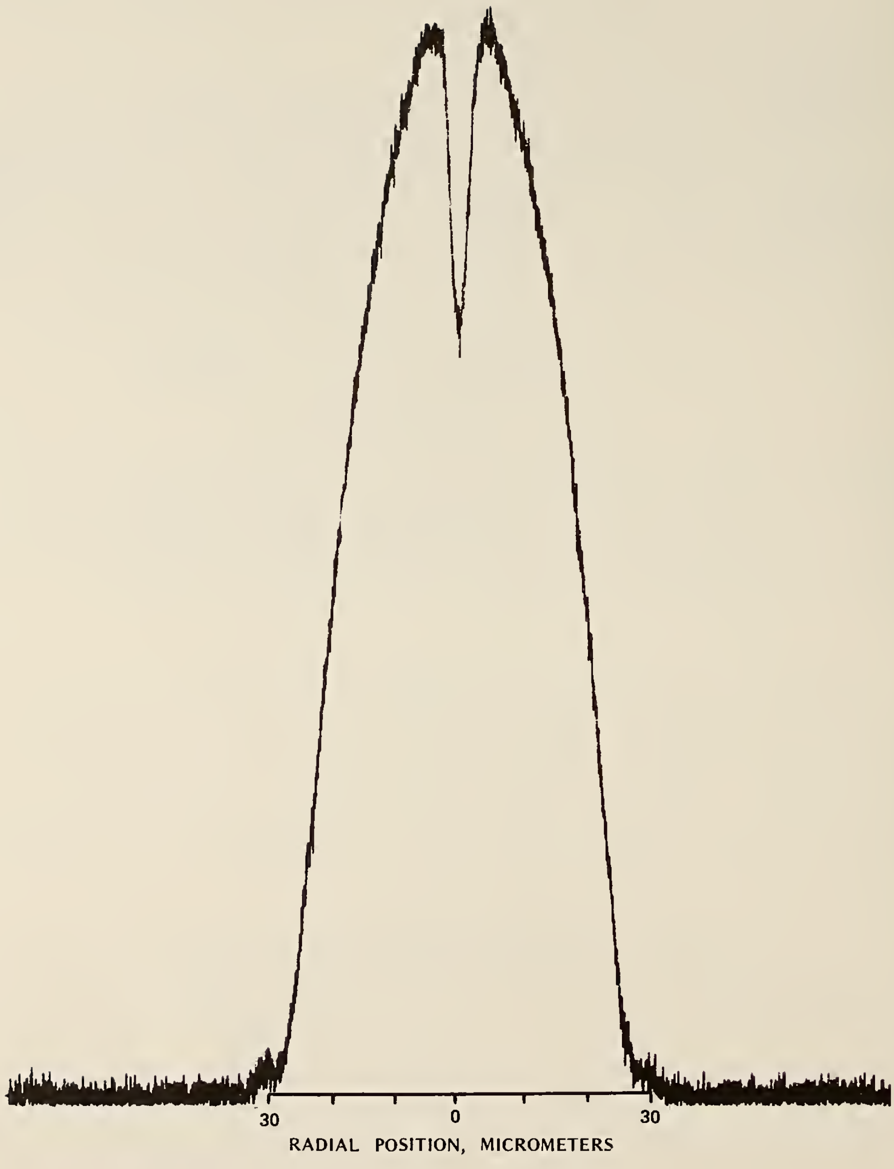

Figure 7-8. Near-field from a 2 m length of graded index fiber with source attenuated by 22 dB. Signal-to-noise ratio of this figure is 17 dB.

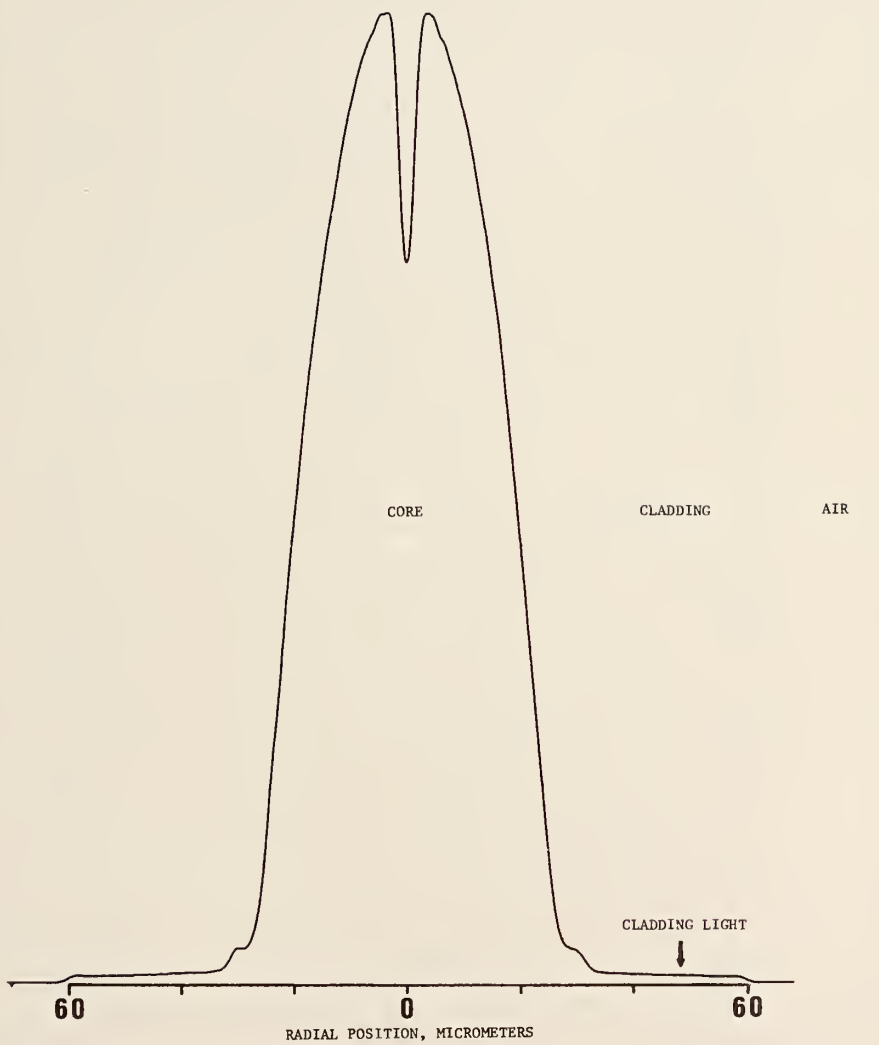

Figure 8-1. Near-field scan across a fiber diameter including the core and cladding regions to observe light in the cladding region.

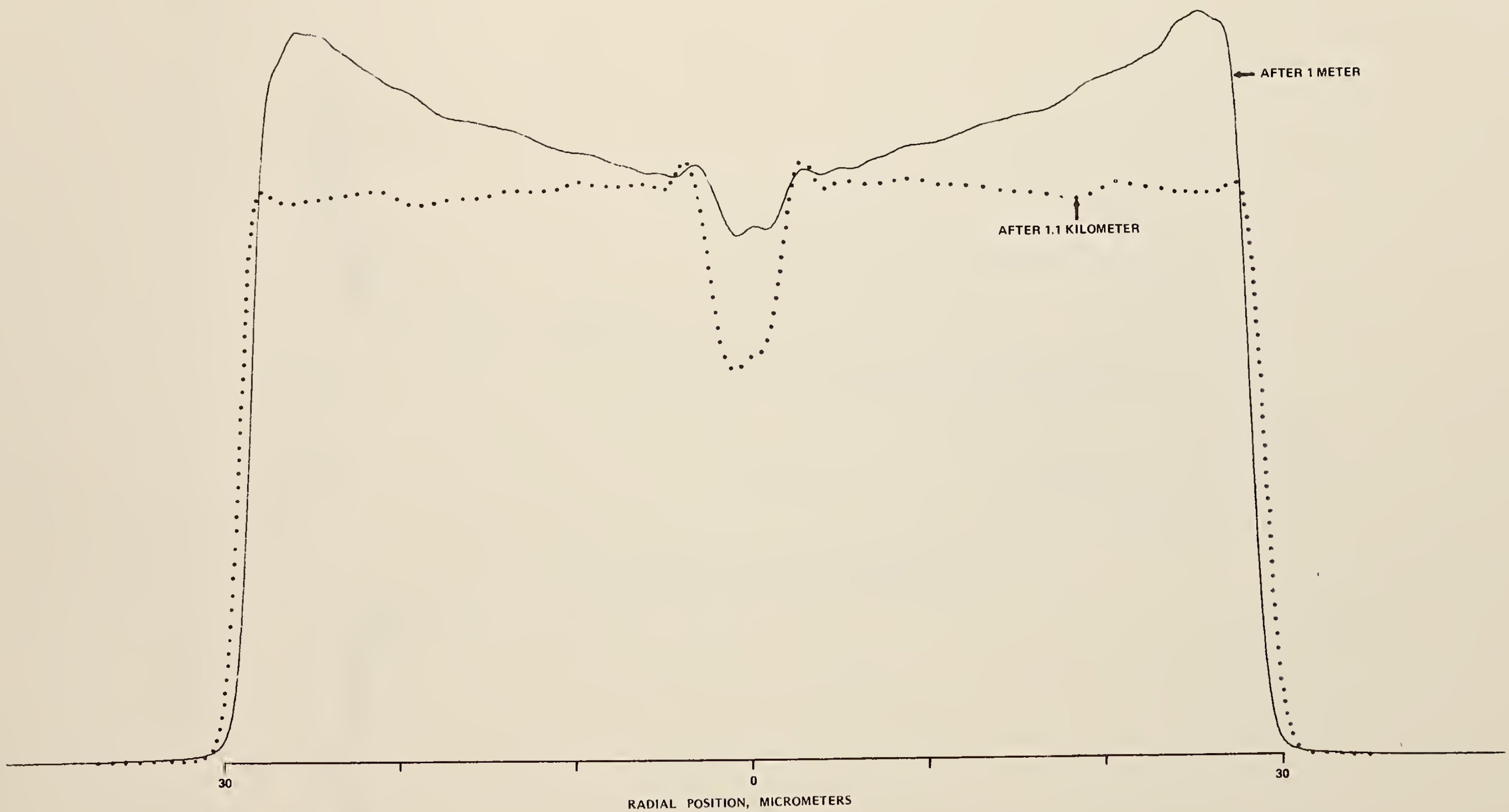

Figure 8-2. Example of the affect of leaky modes on the near-field pattern from a short length of step index fiber. After 1.1 km most leaky modes have been attenuated.

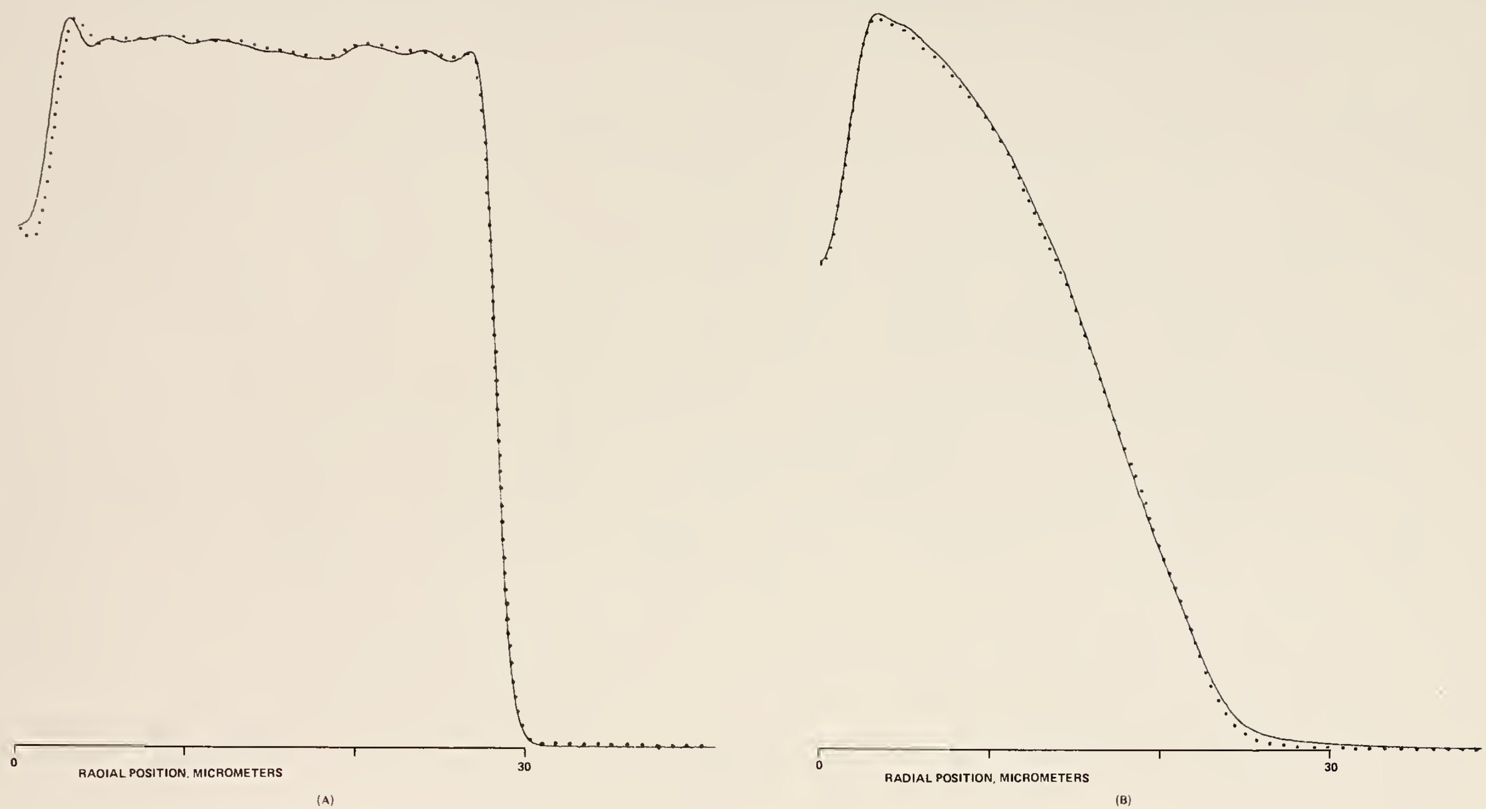

Figure 8-3. Typical symmetry of near-field patterns. Left part of pattern (dotted line) is folded about a vertical axis through mid-point of half maximum width to compare with right part of pattern (solid line).

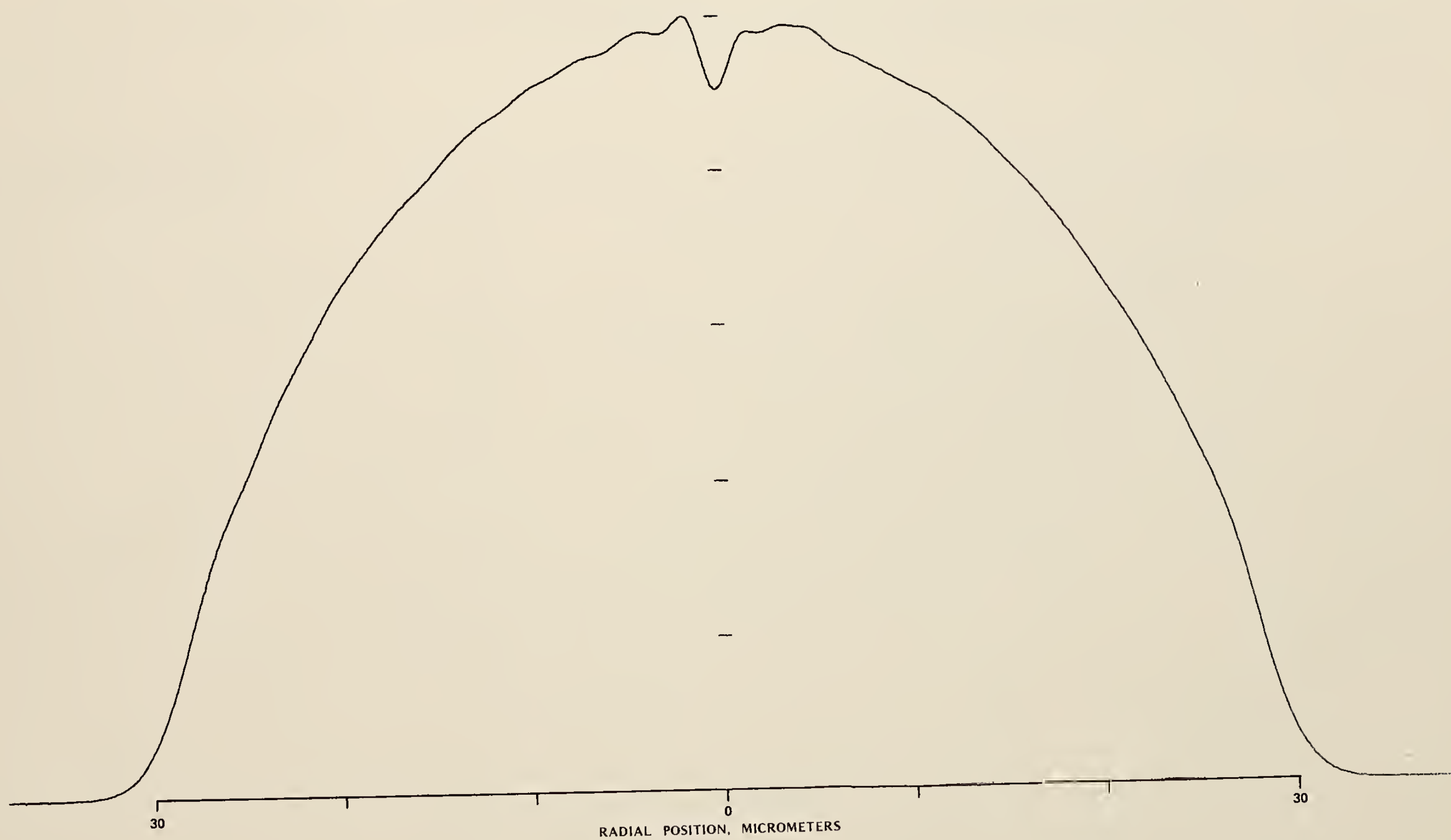

Figure 8-4. Example of a small on-axis index dip obtained from a fiber made by the outside vapor phase oxidation process.

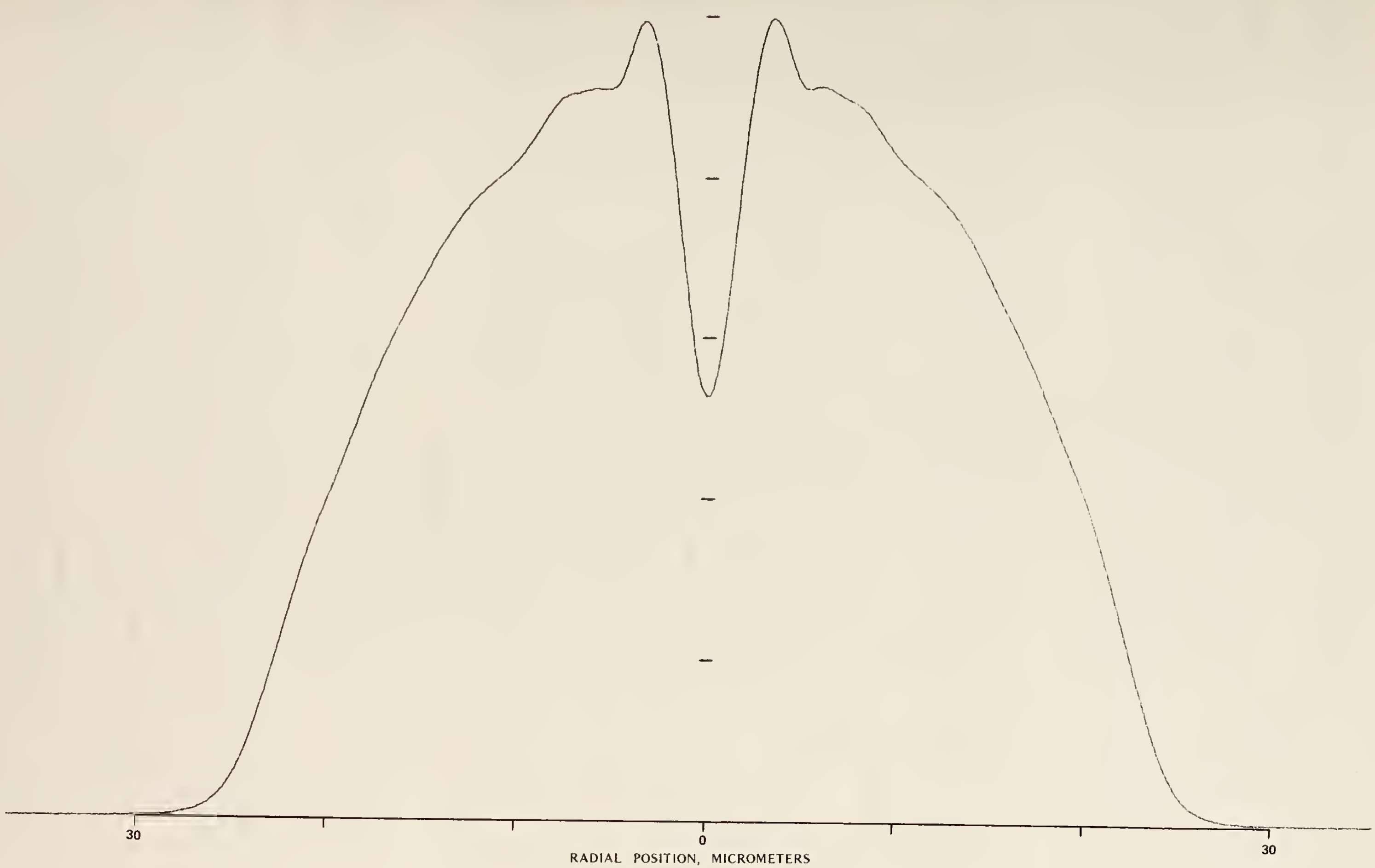

Figure 8-5. Example of a rather large on-axis index dip obtained from a graded index fiber.

intended to show the diverse behavior of index dips found in commercially available graded index fibers.

The outside chemical vapor deposition process generally gives smaller dips than the inside process. Figure 8-4 is an example of a fiber made by an outside process and exhibits the smallest dip we have observed.

Figure 8-5 shows the largest dip observed with the system to date. The depth is about half of the peak height of the curve. In many of the index dips measured, the widths are close to the system resolution. Consequently, the dips are deeper than the near-field measurements indicate. Other methods for determining index profile such as refracted near field offer better resolution for these kinds of measurement.

9. CONCLUSION

The determination of radiation angle (numerical aperture) from far-field data at the 5 percent intensity points should result in good measurement precision and accuracy when applied to near-parabolic, index fibers. In these fibers, leaky modes are contained within the meridionally defined numerical aperture so they should not affect the intensity at the largest observed angles. However, in step index fibers the situation is different. Here leaky modes cause uncertainty if meridionally defined numerical aperture is desired. At present, standards groups have not made recommendations for step index fibers.

More work is needed if core diameter is to be determined from a near-field measurement. Correlation between the near field and index profile at the core-cladding boundary must be established. The use of a low index "barrier layer" may cause differences between core diameter determined by near-field and index profile measurements. By judiciously choosing definitions, it should be possible to reduce systematic errors between these two measurements. Technically, near-field measurements are much easier to impliment than index profile measurements which, for the most part, rely on interferometry over small dimensions.

10. REFERENCES

[1] Cathey, W. T. Optical information processing and holography. New York:John Wiley; 1974.

[2] Sladen, F. M. E., et al. Determination of optical fiber refractive index profiles by a near-field scanning technique. A.P.L. 28(5):255-258; 1976 March.

[3] Adams, M. J., et al. Leaky rays on optical fibers of arbitrary (circularly symmetric) index profiles. Electronics Letters, 11(11):239-240; 1975 May.

[4] Holmes, G. T. Propagation parameter measurements of optical waveguides. Proceedings of the SPIE, Fiber Optics for Communication and Control, Vol. 224; 1980.

[5] Kitayama, K., et al. Impulse response prediction based on experimental mode coupling coefficient in a 10-km long graded-index fiber. IEEE J. Quant. Elect. QE-16(3):356-362; 1980 March.

[6] Procedures for determining radiation angle (numerical aperture) and core diameter from far and near-field patterns respectively are under consideration by Committee P6.6 of the Electronic Industries Association.

[7] Hanson, A. G., et al. Optical waveguide communications glossary. NTIA Special publication, NTIA-SP-79-4; 1979 September.

[8] Electronics Industries Association Committee P6.6 is currently recommending that radiation angle be based on the far-field pattern half width at the 5 percent intensity points.

[9] Miller, S. E.; Chynoweth, A. G. Optical Fiber Telecommunications. New York:Academic Press; 1979.

[10] Matsumura, H. The light acceptance angle of a graded index fibre. Optical and Quantum Electronics 7:81-86; 1975.

[11] Eriksrud, M., et al. Comparison between measured and predicted transmission characteristics of 12 km spliced graded-index fibres. Optical and Quantum Electronics. 11:517-523; 1979.

[12] Tateda, M. Optical loss measurements in graded-index fiber using a dummy fiber. Applied Optics. 18(19):3272-3275; 1979 October.

[13] Cherin, A. H.; Gardner, W. B. Standardization of optical fiber transmission measurements. Laser Focus. 16(8):60-65; 1980 August.

[14] Adams, M. J., et al. Length-dependent effects due to leaky modes on multimode graded-index optical fibres. Optics Communications. 17(2):204-209; 1976 May.

[15] Petermann, K. Uncertainties of the leaky mode correction for near-square-law optical fibres. Electronics Letters. 13(17):513-514; 1977 August.

[16] Barrell, K. F.; Pask, C. Leaky ray correction factors for elliptical multimode fibres. Electronics Letters. 16(14):532-533; 1980 July.

[17] Hazan, J. P. Intensity profile distortion due to resolution limitation in fibre index profile determination by near field. Electronics Letters. 14(5):158-160; 1978 March.

[18] Sabine, P. V. H., et al. Fibre refractive-index profiling by modified near-field scanning. Electronics Letters. 16(23):882-883; 1980 November.

[19] Sladen, F. M. E., et al. Measurement of profile dispersion in optical fibers: a direct technique. Electronics Letters. 13(7):212-213; 1977 February.

[20] PIN photodiodes with built-in operational amplifiers are available from a number of sources. A 22 megohm feedback resistor is used with the operational amplifier.

[21] The alphabetical fiber designations are consistent within this Technical Note but do not apply to any other NBS publications.

[22] Gloge, D.; Marcatili, E. A. J. Multimode theory of graded-core fibers. B.S.T.J. 52(9):1563-1578; 1973 November.

[23] Tokuda, M., et al. Measurement of baseband frequency response of multimode fibre by using a new type of mode scrambler. Electronic Letters. 13(5):146-147; 1977 March.

[24] Franzen, D. L.; Day, G. W. Measurement of optical fiber bandwidth in the time domain. Nat. Bur. Stand. (U.S.) Tech. Note 1019; 1980 February.

[25] Conduit, A. J., et al. Spectral and length-dependent losses in optical fibres investigated by a two-channel backscatter technique. Electronics Letters. 16(3): 77-78; 1980 January.

[26] Born, M.; Wolf, E. Principles of Optics. New York:Pergamon Press; 1964.

[27] Adams, M. J., et al. Resolution limit of the near-field scanning technique. Proceedings of the Third European Conf. Opt. Comm.; 1977; Munich.

[28] Eickhoff, W.; Krumpholtz, O. Pulse response and microbending losses of an optical glass-fibre waveguide with a bump in its index profile. Electronics Letters. 13(9):256-257; 1977 April.

NBS-114A (REV. 2-80)

U.S. DEPT. OF COMM. BIBLIOGRAPHIC DATA SHEET (See instructions)	1. PUBLICATION OR REPORT NO. NBS TN-1032	2. Performing Organ. Report No.	3. Publication Date March 1981

4. TITLE AND SUBTITLE

Measurement of Far-Field and Near-Field Radiation Patterns from Optical Fibers

5. AUTHOR(S)

Ernest M. Kim and Douglas L. Franzen

6. PERFORMING ORGANIZATION (If joint or other than NBS, see instructions)

NATIONAL BUREAU OF STANDARDS
DEPARTMENT OF COMMERCE
WASHINGTON, D.C. 20234

7. Contract/Grant No.

8. Type of Report & Period Covered

9. SPONSORING ORGANIZATION NAME AND COMPLETE ADDRESS (Street, City, State, ZIP)

Supported in part by the Department of Defense, Calibration Coordination Group (CCG).

10. SUPPLEMENTARY NOTES

[ ] Document describes a computer program; SF-185, FIPS Software Summary, is attached.

11. ABSTRACT (A 200-word or less factual summary of most significant information. If document includes a significant bibliography or literature survey, mention it here)

Systems are described for measuring the far- and near-field radiation patterns from optical fibers. Parameters which affect measurement precision, accuracy, resolution, and signal-to-noise ratio are discussed. Measurements utilizing radiation patterns are covered; this includes radiation angle (numerical aperture), attenuation using mode filters, index profile, core diameter, and mode volume transfer function. Experimental examples are given in many instances.

12. KEY WORDS (Six to twelve entries; alphabetical order; capitalize only proper names; and separate key words by semicolons)

Attenuation; core diameter; far field; index profile; mode filter; numerical aperture; radiation angle; radiation patterns.

13. AVAILABILITY

[x] Unlimited
[ ] For Official Distribution. Do Not Release to NTIS
[x] Order From Superintendent of Documents, U.S. Government Printing Office, Washington, D.C. 20402.
[ ] Order From National Technical Information Service (NTIS), Springfield, VA. 22161

14. NO. OF PRINTED PAGES

48

15. Price

$2.50

NBS TECHNICAL PUBLICATIONS

PERIODICALS

JOURNAL OF RESEARCH—The Journal of Research of the National Bureau of Standards reports NBS research and development in those disciplines of the physical and engineering sciences in which the Bureau is active. These include physics, chemistry, engineering, mathematics, and computer sciences. Papers cover a broad range of subjects, with major emphasis on measurement methodology and the basic technology underlying standardization. Also included from time to time are survey articles on topics closely related to the Bureau's technical and scientific programs. As a special service to subscribers each issue contains complete citations to all recent Bureau publications in both NBS and non-NBS media. Issued six times a year. Annual subscription: domestic $13; foreign $16.25. Single copy, $3 domestic; $3.75 foreign.

NOTE: The Journal was formerly published in two sections: Section A "Physics and Chemistry" and Section B "Mathematical Sciences."

DIMENSIONS/NBS—This monthly magazine is published to inform scientists, engineers, business and industry leaders, teachers, students, and consumers of the latest advances in science and technology, with primary emphasis on work at NBS. The magazine highlights and reviews such issues as energy research, fire protection, building technology, metric conversion, pollution abatement, health and safety, and consumer product performance. In addition, it reports the results of Bureau programs in measurement standards and techniques, properties of matter and materials, engineering standards and services, instrumentation, and automatic data processing. Annual subscription: domestic $11; foreign $13.75.

NONPERIODICALS

Monographs—Major contributions to the technical literature on various subjects related to the Bureau's scientific and technical activities.

Handbooks—Recommended codes of engineering and industrial practice (including safety codes) developed in cooperation with interested industries, professional organizations, and regulatory bodies.

Special Publications—Include proceedings of conferences sponsored by NBS, NBS annual reports, and other special publications appropriate to this grouping such as wall charts, pocket cards, and bibliographies.

Applied Mathematics Series—Mathematical tables, manuals, and studies of special interest to physicists, engineers, chemists, biologists, mathematicians, computer programmers, and others engaged in scientific and technical work.

National Standard Reference Data Series—Provides quantitative data on the physical and chemical properties of materials, compiled from the world's literature and critically evaluated. Developed under a worldwide program coordinated by NBS under the authority of the National Standard Data Act (Public Law 90-396).

NOTE: The principal publication outlet for the foregoing data is the Journal of Physical and Chemical Reference Data (JPCRD) published quarterly for NBS by the American Chemical Society (ACS) and the American Institute of Physics (AIP). Subscriptions, reprints, and supplements available from ACS, 1155 Sixteenth St., NW, Washington, DC 20056.

Building Science Series—Disseminates technical information developed at the Bureau on building materials, components, systems, and whole structures. The series presents research results, test methods, and performance criteria related to the structural and environmental functions and the durability and safety characteristics of building elements and systems.

Technical Notes—Studies or reports which are complete in themselves but restrictive in their treatment of a subject. Analogous to monographs but not so comprehensive in scope or definitive in treatment of the subject area. Often serve as a vehicle for final reports of work performed at NBS under the sponsorship of other government agencies.

Voluntary Product Standards—Developed under procedures published by the Department of Commerce in Part 10, Title 15, of the Code of Federal Regulations. The standards establish nationally recognized requirements for products, and provide all concerned interests with a basis for common understanding of the characteristics of the products. NBS administers this program as a supplement to the activities of the private sector standardizing organizations.

Consumer Information Series—Practical information, based on NBS research and experience, covering areas of interest to the consumer. Easily understandable language and illustrations provide useful background knowledge for shopping in today's technological marketplace.

Order the **above** *NBS publications from: Superintendent of Documents, Government Printing Office, Washington, DC 20402.*

Order the **following** *NBS publications—FIPS and NBSIR's—from the National Technical Information Services, Springfield, VA 22161.*

Federal Information Processing Standards Publications (FIPS PUB)—Publications in this series collectively constitute the Federal Information Processing Standards Register. The Register serves as the official source of information in the Federal Government regarding standards issued by NBS pursuant to the Federal Property and Administrative Services Act of 1949 as amended, Public Law 89-306 (79 Stat. 1127), and as implemented by Executive Order 11717 (38 FR 12315, dated May 11, 1973) and Part 6 of Title 15 CFR (Code of Federal Regulations).

NBS Interagency Reports (NBSIR)—A special series of interim or final reports on work performed by NBS for outside sponsors (both government and non-government). In general, initial distribution is handled by the sponsor; public distribution is by the National Technical Information Services, Springfield, VA 22161, in paper copy or microfiche form.

U.S. DEPARTMENT OF COMMERCE
National Bureau of Standards
Washington, D.C. 20234

OFFICIAL BUSINESS

Penalty for Private Use, $300

POSTAGE AND FEES PAID
U.S. DEPARTMENT OF COMMERCE
COM-215

U.S.MAIL

SPECIAL FOURTH-CLASS RATE
BOOK